PMEL Tsunami Forecast Series: XX

Development of a Tsunami Forecast Model for Montauk, New York

Edison Gica

March 16, 2015

Table of Contents

List of Tables

List of Figures

PMEL Tsunami Forecast Series: Vol. XX
Development of a Tsunami Forecast Model for Montauk, New York, USA

Abstract:

The National Oceanic and Atmospheric Administration has developed a tsunami forecast model for Montauk, New York, as part of an effort to provide tsunami forecasts for United States coastal communities. Development, validation, and stability testing of the tsunami forecast model has been conducted to ensure model robustness and stability. The Montauk tsunami forecast model employs the Method of Splitting Tsunami numerical code and the stability and reliability was tested by simulating historical events and artificial mega-tsunamis from different source regions. The 1755 Lisbon tsunami was simulated for the historical event. A total of 8 synthetic mega tsunami (6 Mw 9.3, 1 Mw 7.5 and 1 Mw 6.2) were used and the forecast model was stable for 24 hours. The Montauk forecast model can generate 4 hr of tsunami wave characteristics in approximately 5.85 min of CPU time.

1.0 Background and Objectives

The National Oceanic and Atmospheric Administration (NOAA) Center for Tsunami Research (NCTR) at the NOAA Pacific Marine Environmental Laboratory (PMEL) has developed a tsunami forecasting capability for operational use by NOAA's two Tsunami Warning Centers located in Hawaii and Alaska (Titov *et al.*, 2005). The system is designed to efficiently provide basin-wide warning of approaching tsunami waves accurately and quickly. The system, termed Short-term Inundation Forecast of Tsunamis (SIFT), combines real-time tsunami event data with numerical models to produce estimates of tsunami wave arrival times and amplitudes at a coastal community of interest. The SIFT system integrates several key components: deep-ocean observations of tsunamis in real time, a basin-wide pre-computed propagation database of water level and flow velocities based on potential seismic unit sources, an inversion algorithm to refine the tsunami source based on deep-ocean observations during an event, and high-resolution tsunami forecast models.

Montauk is in the eastern part of Long Island, New York, and approximately 100 miles east of New York City (Figure 1). Boasting pristine white beaches and acres of diverse parkland, Montauk covers 19.8 sq mi (Montauk Chamber of Commerce, 2013)which encompasses a variety of habitat: maritime beaches, dunes, forests (coastal and maritime), grasslands, shrublands and wetlands (fresh, salt and brackish) (The Nature Conservancy, 2013). Montauk was occupied by Native Americans when the first Europeans arrived in early 1600s. Montauk Sachem ruled the Native Americans from Montauk to the west end of the island. The principal village was located at Fort Pond (Figure 2) which is near Montauk Point. The Europeans were a group of English men and women from Massachusetts who purchased land in 1648 from the Montauk Indians that spanned Southampton's eastern boundary to Napeague Beach.

As of 2010, the total population is 3,326 (Census 2010) with a median household income of $71,593, a mean household income of $97,749 and a per capita income of $47,446. The occupation of the population is in management, business, science and arts at 31.3%; service at

23.9%; sales and office at 23.1%; natural resources, construction and maintenance covering 17.1%; and production, transportation and material moving occupying 4.5%. Based on American Community Survey 5-year estimates (2007-2011), the top three industries are arts, entertainment, recreation, accommodation and food services covering 19.7%; educational services, health care and social assistance at 12.8%; and construction at 15.1% (Census 2010). Tourist attractions in Montauk include whale watching, fishing and bird watching. One can visit the oldest intact building in Montauk, the Second House Museum (erected in 1700), and the oldest lighthouse in the state of New York, the Montauk Point Lighthouse completed in 1796 (Montauk Lighthouse, 2013)

To protect life and property, Montauk was selected by the Tsunami Warning Centers as part of the 75 tsunami forecast models that will be developed for the United States coastlines and territories. This report details the development of a tsunami forecast model for Montauk. Development includes construction of a digital elevation model based on available bathymetric and topographic data, model validation with historic events, and stability tests of the model with a suite of mega-tsunami events originating from subduction zones in the Caribbean.

The initial development of the Montauk inundation forecast model was done by Wilford E. Schmidt back in September 2009 (personal communication). Sometime in 2010, NCTR generated a standard list of synthetic scenarios to test the stability and reliability of the forecast model being developed. Using the new list of synthetic scenarios, it was found that the forecast model generated localized instabilities. Corrections on the digital elevation model were made to address those issues.

2.0 Forecast Methodology

A high-resolution inundation model was used as the basis for development of a tsunami forecast model to operationally provide an estimate of wave arrival time, wave height and inundation at Montauk following tsunami generation. All tsunami forecast models are run in real time while a tsunami is propagating across the open ocean. The Montauk model was designed and tested to perform under stringent time constraints given that time is generally the most important limiting factor in saving lives and property. The goal of this work is to maximize the length of time that the community of Montauk has to react to a tsunami threat by providing accurate information quickly to emergency managers and other officials responsible for the community and infrastructure.

The general tsunami forecast model, based on the Method of Splitting Tsunami (MOST), is used in the tsunami inundation and forecasting system to provide real-time tsunami forecasts at selected coastal communities. The model runs in minutes while employing high-resolution grids constructed by the National Geophysical Data Center. The MOST is a suite of numerical simulation codes capable of simulating three processes of tsunami evolution: earthquake, transoceanic propagation and inundation of dry land. The MOST model has been extensively tested against a number of laboratory experiments and benchmarks (Synolakis *et al.*, 2008) and was successfully used for simulations of many historical tsunami events. The main objective of a forecast model is to provide an accurate, yet rapid, estimate of wave arrival time, wave height and inundation in the minutes following a tsunami event. Titov and González (1997) describe the

technical aspects of forecast model development, stability, testing and robustness while Tang *et al*., 2009 provide detailed forecast methodology

A basin-wide database of pre-computed water elevations and flow velocities for unit sources covering worldwide subduction zones has been generated to expedite forecasts (Gica *et al.*, 2008). As the tsunami wave propagates across the ocean and successively reaches tsunameter observation sites, recorded sea level is ingested into the tsunami forecast application in near real-time and incorporated into an inversion algorithm to produce an improved estimate of the tsunami source. A linear combination of the pre-computed database is then performed based on this tsunami source, now reflecting the transfer of energy to the fluid body, to produce synthetic boundary conditions of water elevation and flow velocities to initiate the forecast model computation.

Accurate forecasting of the tsunami impact on a coastal community largely relies on the accuracies of bathymetry and topography and the numerical computation. The high spatial and temporal grid resolution necessary for modeling accuracy poses a challenge in the run-time requirement for real-time forecasts. Each forecast model consists of three telescoped grids with increasing spatial resolution in the finest grid, and temporal resolution for simulation of wave inundation onto dry land. The forecast model utilizes the most recent bathymetry and topography available to reproduce the correct wave dynamics during the inundation computation. Forecast models, including the Montauk model, are constructed for at-risk populous coastal communities in the Pacific and Atlantic Oceans. Previous and present development of forecast models in the Pacific (Titov *et al*., 2005; Titov, 2009; Tang *et al*., 2009; Wei *et al*., 2008) have validated the accuracy and efficiency of each forecast model currently implemented in the real-time tsunami forecast system. Models are tested when the opportunity arises and are used for scientific research.

3.0 Model Development

The general methodology for modeling at-risk coastal communities is to develop a set of three nested grids, referred to as A, B, and C-grids, each of which becomes successively finer in resolution as they telescope into the population and economic center of the community of interest. The offshore area is covered by the largest coverage area and lowest resolution A grid while the near-shore details are resolved within the finest scale C grid to the point that tide gauge observations recorded during historical tsunamis are resolved within expected accuracy limits. The procedure is to begin development with bathymetric and topographic grids at high resolution, and then optimize these grids by sub-sampling to coarsen the resolution and reduce the overall grid dimensions to achieve a 4-hr simulation of modeled tsunami waves within the required time period of 10 min of wall-clock time. The basis for these grids is a high-resolution 1/3-arc-sec Digital Elevation Model (DEM) (Figure 2) constructed by the National Geophysical Data Center (NGDC, 2005; Taylor et al., 2007) using all available bathymetric, topographic, and shoreline data to reproduce the wave dynamics during the inundation computation for an at-risk community. For each community, data are compiled from a variety of sources to produce a DEM referenced to Mean High Water in the vertical and to the World Geodetic System 1984 in the horizontal (NGDC, 2005). The author considers it to be an adequate representation of the local

topography/bathymetry. As new digital elevation models become available, forecast models will be updated and report updates will be posted at http://nctr.pmel.noaa.gov/forecast_reports/. From these digital elevation models, a set of three high-resolution, 'reference' elevation grids are constructed for development of a high-resolution reference model from which an 'optimized' model is constructed to run in an operationally specified period of time. The operationally developed model is referred to as the forecast model.

Development of a forecast model for Montauk began with the bathymetric/topographic grids shown in Figure 2. Grid dimension extension and additional information were updated as needed and appropriate. A significant portion of the modeled tsunami waves, 24 hours of modeled tsunami time for Montauk should pass through the model domain without appreciable signal degradation. Table 1 provides specific details of both reference model and forecast model grids, including extents and complete input parameter information for the model runs provided in Appendix A. Figures 3 and 4 plots the extents of grids A, B and C for the reference and forecast models, respectively.

3.1 Forecast Area

Montauk is in the eastern part of Long Island, New York, and approximately 100 miles east of New York City (Figure 1), covering an area of 19.8 square miles. According to NOAA (Tides and Currents, 2013), the gauge sensor and instrument housing are located in the NE corner of the Rough Rider Condominium Pier, located on the coastal area north of Fort Pond (Figure 5). Due to its location on a wide continental shelf of the U.S. East Coast, the offshore region has a relatively mild slope including the northern side of Montauk, as shown in the contour plotted in Fig. 4c. One advantage of the existence of a wide continental shelf is that it slows down the propagating tsunami wave, dissipating potentially destructive energy and giving adequate time for evacuation.

Most of the populated area is situated at a higher elevation. The lower elevation areas are located on the sandy beach along Atlantic Ocean. For the forecast model, Fort Pond was removed and replaced with 1 cm of land elevation to maintain stability in the simulation. As seen in Figure 4c, the elevation of 5 m is very close to the coastline where the slope quickly rises to 10 m on the hilly areas. In the vicinity of Fort Pond, land elevation is below the 5-m mark. The highest elevation on land is about 58.5 m on the hill west of Fort Pond.

3.2 Historical events and data

In the Atlantic Basin, the Azores-Gibraltar plate boundary located in the Northern Basin is the likely source for the largest earthquake and tsunamis that could potentially affect the U.S. East Coast. Historically, the largest tsunamigenic earthquake that occurred in the Atlantic Ocean was the 1 November 1755 Lisbon earthquake was with an estimated magnitude (Mw) of 8.5 – 9.0 (ten Brink et al., 2008). Fortunately no tsunamigenic earthquake has occurred since then; however, lack of historical observation makes it harder to validate a forecast model for Montauk. This historical tsunami source can still be used to simulate generated tsunami waves and

determine how it might affect Montauk. The location of Montauk relative to the 1755 Lisbon earthquake is shown in Figure 6. Even if there were historical accounts of the 1755 Lisbon tsunami, tide gauge data would not be available since it none were available in Montauk until 5 September 1947. The present installation was established on 21 September 1989.

The tide house is located near a residential development pier on Fort Pond Bay with coordinates of 71° 57.6'W, 41° 2.9'N. The vicinity has a mean tidal range of 0.631 m and a diurnal range of 0.771 m. The station also shows that there is a mean sea level difference of 1.55 m from a record range of 1983–2001 and 1.490 m from 1960–1978 (Tides and Currents, 2013).The closest point selected in the forecast model DEM as the tide gauge location is at 71.96°W, 41.04833294°N with a depth of 5.31 m.

3.3 Model setup

The high-resolution DEM for Montauk was developed by NGDC (Taylor et al., 2007) with a grid resolution of 1/3 arc sec and coverage from 287.4°E to 288.5°E and 40.6°N to 41.4°N (Figure 2). The deepest water depth covered by the domain is 118 m and the highest topography elevation is 162.6 m. The DEM for both B and C grids of the high-resolution reference inundation model and the forecast model was extracted directly from the DEM developed by NGDC. The DEM for the A grid was obtained from a 9-arc-sec grid resolution developed by NGDC for the NOAA Center for Tsunami Inundation Mapping Efforts (TIME). Sources for the 9-arc-sec DEM were obtained from a Smith Global 1-arc-min bathymetry/topography grid, hydrographic survey data (done by National Ocean Service [NOS], Tsunami Warning and Mitigation program, National Geospatial-Intelligence Agency and international surveys), multi-beam data (NOS, Scripps Institution of Oceanography, University of Rhode Island, Woods Hole Oceanographic Institution, Lamont-Doherty Earth Observatory, U.S. Geological Survey and Center for Coastal and Ocean Mapping/Joint Hydrographic Center of the University of New Hampshire), bathymetric contour data (Instituto Nacional de Estadístifica Geographía e Informática), digital coastline data (NOAA Office of Ocean Resources Conservation and Assessment, Strategic Environmental Assessments Division) and bathymetric LIDAR data (Joint Airborne LIDAR Bathymetry Technical Center of Expertise, US Army Corps of Engineers). It should be noted that the 9-arc-sec DEM does not contain topography.

From these two data sources, the nested grids for the forecast and reference models were generated. The extent and grid resolution selected for the reference grid is shown in Table 1. The plots of the nested grid are shown in Figures 3 and 4. The forecast model, which is used for tsunami forecasting during an event, is an optimized version of the high-resolution reference model. It is designed so that it can quickly provide 4 hr of simulated tsunami wave characteristics which includes time series at the warning point. Several grid versions were tested in an attempt to be able to simulate 4 hr of tsunami waves in ~10 min CPU time or less. A quantitative method to assess the "goodness-of-fit" between the reference and optimized warning points time series, the root-mean-square (rms) difference, was computed. An optimized set of grids satisfied the goal of <10 min CPU time, but their resemblance to the reference simulation was unsatisfactory, as judged visually and/or by rms difference. The ultimate solution in this case proved to be maintaining the A and B grid extents of the reference grid with reduced resolution (48 and 18 arc sec, respectively) for the forecast model, and a cropped version of the reference C

grid, also with reduced resolution (6 arc sec). The selected warning point, 288.0399967°E, 41.04833294°N (Figure 3c and 4c), is located near the tide gauge. The water depth of the DEM at this point is 5.31 m.

Due to the complex bathymetry and extremely large tsunami source employed, the resulting simulation was prone to instabilities. Modifications were done on the DEM to make a stable and reliable run. The aim of these modifications was to smooth out the DEM so as to eliminate instabilities. The existence of Fort Pond also generated instability during the testing. This was resolved by removing the water and replacing it with 1 cm of land. This will not affect the solution since the land depth is so shallow that if inundation does occur this area will be quickly flooded. From the stable forecast and reference grids, it takes 5.85 min to simulate a 4-hr tsunami for the forecast grid and 26.82 hr for the reference grid.

4.0 Results and Discussion

The development of the reference and forecast model grids requires that it be validated with historical events and be tested for stability and reliability with synthetic scenarios. The 1755 Lisbon tsunami was used for the historic event and synthetic scenarios used Mw 9.3, Mw 7.5 and a small wave case with Mw 6.2. Validation with historical data is required to determine how well the model predicts the tsunami wave characteristics of actual events. The synthetic scenarios are tested to check whether the reference and forecast models will both produce a stable simulation and will locate possible instabilities in the selected grids. The synthetic mega-event scenarios can also be used as a preliminary risk analysis to determine which tsunami source region poses a threat to Montauk. Tsunami time series at the selected tide gauge and max/min tsunami wave amplitude distribution are also compared between the reference and forecast model grids. This is to check whether the tsunami wave characteristics of the lower-resolution forecast model will not significantly deviate from the reference model grid.

4.1 Model validation

The development of the DEM for the high-resolution reference inundation model and forecast model requires that it be validated to determine the accuracy of the simulated tsunami characteristics as it hits the coastal areas of Montauk. The largest tsunamigenic earthquake to occur in the Atlantic Basin was the 1775 Lisbon. Unfortunately there are no historical data since the earliest tide gauge was not established until 5 September 1947. Also there are no historical accounts of tsunami waves arriving at the coast of Montauk. However, the historical tsunami source (ten Brink et al, 2008) can still be used to determine how the generated tsunami wave would affect the coast of Montauk.

A higher-resolution DEM should provide finer distributions of the tsunami wave pattern which might not be reflected in a forecast model due to a coarser resolution. This is a compromise since the forecast model is designed to provide a quick forecast. However, the deviation with the higher-resolution model should not be too significant. Comparison between the forecast model

and high-resolution model will be evaluated by looking at the tide gauge time series and distribution of the maximum tsunami wave amplitude in grids A, B and C.

4.2 Model stability and reliability

The development of the forecast model requires that the model provide a reliable forecast and be stable enough to simulate several hours of the tsunami event. A set of reliability and stability tests was conducted by simulating synthetic events emanating from different regions and using different earthquake magnitudes (Mw 9.3, 7.5, and 6.2). Since each tsunami event is unique, tests using various earthquake magnitudes and source locations would indicate if the model grid developed will generate instabilities that need to be corrected. This set of tests is not exhaustive. However, representative cases from select sources should be sufficient. A total of six artificial mega-tsunamis (Mw 9.3) were generated from twenty unit sources with a slip value of 25 m for each unit source. One case of Mw 7.5 uses one unit source with a slip of one meter while one case of Mw 6.2 tests the model for a small wave condition. The unit sources are from the propagation database developed at NCTR (Gica et al., 2008). Tests were conducted using a 24-hr simulation for the forecast model and 12 hr for the reference model. The list of sources used is indicated in Table 2 for the artificial mega-tsunamis Mw 7.5 and Mw 6.2. The locations in reference to Montauk are shown in Figure 6.

4.3 Results of tested events

The development of the forecast model and high-resolution model requires that it be compared with historical events for validation. Unfortunately there are no historical records for Montauk even for the 1755 Lisbon tsunami which was documented in Europe. However the historical tsunami source can still be used to simulate the generated tsunami waves and determine how it might affect Montauk. Validation will be done by comparing the simulated tsunami wave characteristics between the forecast model and high-resolution model since it is expected that the higher resolution would provide a finer distribution of tsunami wave patterns. Maximum tsunami wave amplitude plots for grids A, B and C for the historical 1755 Lisbon case compare favorably between the forecast and reference models (Figure 7). A closer look at the C-grid level indicates that the reference model has a higher maximum tsunami wave amplitude distribution along the coast as compared with the forecast model (Figure 8, top). This could be attributed to the higher grid resolution of the reference model resolving more of the tsunami waves in the shallow region. The time series at the selected warning point shows good comparison between the forecast and reference model (Figure 8, bottom). In terms of inundation, the 1755 Lisbon scenario does not affect Montauk. No inundation occurs along the coast of both reference and forecast model C grid with a maximum tsunami amplitude of less than 20 cm at the warning point (Figure 8, bottom).

Similarly, the maximum tsunami wave amplitude plots for the mega-tsunami generated from the Caribbean source region show that overall the reference model has a higher offshore maximum amplitude distribution as compared with the forecast model. This is evident especially at the C-grid level for cases AT38-47ab, AT48-57ab and AT82-91ab. Plots of the maximum tsunami wave amplitude distribution and time series at the selected warning point are shown in Figs. 9 to

20 for grids A, B and C. Of all 6 mega-scenarios simulated, only one scenario, AT48-57ab, generated inundation along the entire coast (facing the Atlantic Ocean) of Montauk. Due to the high waves and low-lying region south of Fort Pond, the propagating tsunami waves spilled into the pond and overflowed into the other side of the peninsula (Figure 12, top). Comparison of the tsunami time series at the selected warning point between the forecast and reference model are relatively good. It should be noted that the reference model was simulated for only 12 hr as compared to 24 hr for the forecast model. Although the reference model did show higher offshore maximum tsunami wave amplitude when compared to the forecast model, the comparisons were consistent in indicating whether inundation occurred or not. The forecast model was shown to be stable for 24 hr of simulation based on 6 mega-event scenarios including the one case of Mw 7.5 and one case of Mw 6.2. As for the reference model, it was tested for a 12-hr simulation for the same cases as the forecast model and results indicate that it is relatively stable. Although the tsunami time series at the warning point does show some high-frequency waves at a later time for some cases. However, this probable localized instability does not contaminate the entire solution and does not significantly affect the propagating tsunami waves and prediction of inundation.

Although the suite of simulated mega-tsunamis is not comprehensive, results do indicate that an Mw 9.3 originating along the AT48-57 case pose a threat for Montauk. The impact of case AT48-57ab is more significant as compared with the historic 1755 Lisbon scenario. The maximum tsunami amplitude generated by AT48-57ab is close to 3 m while the 1755 Lisbon scenario is less than 20 cm. This is attributed to the orientation of the earthquake fault since unit sources along the AT48-57 directly face Montauk as opposed to the differing orientation of the 1755 Lisbon scenario. Also, due to the bathymetry of the continental shelf and its orientation, the incoming tsunami waves focus and defocus as they traverse the continental shelf. In some case scenarios simulated (e.g. AT48-57ab), the tsunami waves focus toward Montauk. This study of wave focusing and defocusing for the U.S. Atlantic coast was done by Gica et al. (2012).

5.0 Summary and Conclusion

A set of high-resolution and forecast inundation models has been prepared for Montauk. During development, instabilities occurred and these locations were corrected manually or by smoothing a cluster of nodes if the single node causing the instability was not located. Another correction was to convert Fort Pond to a very low-lying land area with an elevation of 1 cm. Although there were corrections made to the DEM, both models were found to be reliable and the comparison between the high-resolution model and forecast model showed relatively good comparison at the tide gauge station and the distribution of the maximum tsunami wave amplitude in all the grids (i.e. grids A, B and C). However, the reference grid generally produced a higher maximum tsunami wave amplitude distribution as compared to the forecast model.

The stability tests show that the forecast model is stable for a 24-hr simulation for synthetic sources with different earthquake magnitudes (Mw 9.3, 7.5, and 6.2) from different source regions. Six Mw 9.3, one Mw 7.5 and one Mw 6.2 were simulated. The synthetic mega-tsunamis not only check the stability of the forecast model, it can also provide information on which earthquake source regions pose the greatest tsunami threat to Montauk. From the tests conducted,

mega-event case AT48-57ab generates inundation along the coast (facing the Atlantic Ocean). It should be emphasized that this is based on a very limited set of mega-tsunamis. Additionally, mega-tsunamis along the AT48-57 source could also affect the coastal areas. Simulation of a 1755 Lisbon scenario did not affect the coastal areas of Montauk and the maximum tsunami wave amplitude at the selected warning point was less than 20 cm.

Since the main objective of developing the Montauk forecast model is for tsunami forecast, the DEM has been optimized to simulate 4 hr of tsunami wave characteristics in approximately 5.85 min. As presented in this report, the Montauk forecast model can provide a reliable forecast during an event and is stable for a 24-hr simulation.

6.0 Acknowledgements

This work is funded by the Joint Institute for the Study of the Atmosphere and Ocean (JISAO) under NOAA Cooperative Agreement Numbers NA10OAR4320148 and NA08OAR4320899 and is JISAO contribution number No. 2115. This work is also Contribution No. 3370 from NOAA/Pacific Marine Environmental Laboratory. The author would also like to thank Lindsey Wright (for retrieving historical tide gauge data and testing of the forecast model in SIFT as reported in Appendix C) and Sandra Bigley (for comments, edits and formatting of this report).

7.0 References

Census, U.S. Census Bureau 2010, factfinder2.census.gov, accessed 22 March 2013.

Gica, Edison, M.C. Spillane, V.V. Titov, C.D. Chamberlin and J.C. Newman (2008): Development of the forecast propagation database for NOAA's Short-term Inundation Forecast for Tsunamis (SIFT), NOAA Tech. Memo OAR PMEL139, NOAA/Pacific Marine Environmental Laboratory, Seattle, WA, 89pp.

Gica, Edison, M.C. Spillane and V.V. Titov (2012): Chapter 1, Regional (U.S. East Coast) Earthquake Hazard, Tsunami Hazard Assessment for the U.S. East Coast Based on Generation, Propagation and Inundation Modeling, Office of Nuclear Regulatory Research, Division of Engineering [in-press].

Montauk Chamber of Commerce, www.montaukchamber.com, accessed 20 March 2013.

Montauk Lighthouse, www.montauklighthouse.com, accessed 20 March 2013.

National Geophysical Data Center (2005): East Coast and Gulf Coast and Caribbean Nine Second Tsunami Propagation Grids Compilation Report, 1 Dec 2005.

On Montauk, www.onmontauk.com, accessed 26 March 2013.

Synolakis, C.E., E.N. Bernard, V.V. Titov, U. Kânoğlu and F.I. González (2008): Validation and verification of tsunami numerical models. *Pure and Applied Geophysics* 165(11-12), 2197-2228.

Tang, L., V.V. Titov, and C.D. Chamberlin (2009): Development, testing, and applications of site-specific tsunami inundation models for real-time forecasting. *J. Geophys. Res.*, 6, doi: 10.1029/2009JC005476, in press.

Taylor, L.A., B.W. Eakins, K.S. Carignan, R.R. Warnken, T. Sazonova, and D.C. Schoolcraft (2007), Digital Elevation Model for Montauk, New York: Procedures, Data Sources and Analysis, NOAA National Geophysical Data Center, September 28, 2007.

Ten Brink, U., Twichell, D., Geist, E., Chaytor, J., Locat, J., Lee, H., Buczkowski, B., Barkan, R., Solow, A., Andrews, B., Parsons, T., Lynett, P., Lin, J., and Sansoucy, M. (2008): Evaluation of Tsunami Sources with the Potential to Impact the U.S. Atlantic and Gulf Coasts, An Updated Report to the Nuclear Regulatory Commission, by the Atlantic and Gulf of Mexico Tsuanmi Hazard Assessment Group, revised August 22, 2008.

Tides and Currents, http://tidesandcurrents.noaa.gov/datums.html?id=8510560, accessed 20 March 2013.

Titov, V.V. and F.I. Gonzalez (1997): Implementation and testing of Method of Splitting Tsunami (MOST) model. NOAA Tech. Memo. ERL PMEL-112 (PB98-122773), NOAA/Pacific Marine Environmental Laboratory, Seattle, WA, 11pp.

Titov, V.V., F.I. Gonzalez, E.N. Bernard, M.C. Eble, H.O. Mofjeld, J.C. Newman and A.J. Venturato (2005): Real-time tsunami forecasting: Challenges and solutions. Natural Hazards, 35, 41-58.

Titov, V.V. (2009): Tsunami forecasting. In *The Sea*, Vol. 15, Chapter 12, Harvard University Press, Cambridge, MA, and London, England, 371–400.

Wei, Y., E. Bernard, L. Tang, R. Weiss, V. Titov, C. Moore, M. Spillane, M. Hopkins, and U. Kâno˘glu (2008): Real-time experimental forecast of the Peruvian tsunami of August 2007 for U.S. coastlines. *Geophys. Res. Lett.*, *35*, L04609, doi: 10.1029/2007GL032250.

Table 1: MOST setup parameters for reference and forecast models for Montauk, New York.

		Reference Model				Forecast Model			
Grid	Region	Coverage Lat. [ºN] Lon. [ºW]	Cell Size [“]	nx x ny	Time Step [sec]	Coverage Lat. [ºN] Lon. [ºW]	Cell Size [“]	nx x ny	Time Step [sec]
A	New York Bight	38.0000-41.4999 71.0000-75.0000	12	1201 x 1051	1.2	17.6540-18.7310 65.0660-67.9470	48	301 x 341	4.0
B	Eastern Long Island	40.8000-41.2000 71.8000-72.2000	6	721 x 721	1.2	40.8000-41.1999 71.8000-72.2000	18	161 x 241	4.0
C	Montauk	40.9100-41.0900 71.9100-72.0900	1	1945 x 1945	0.3	40.9750-41.0877 71.9150-72.0200	6	301 x 508	2.0
Minimum offshore depth [m]				5.0				5.0	
Water depth for dry land [m]				0.1				0.1	
Friction coefficient [n^2]				0.0009				0.0009	
CPU time for 4-hr simulation				26.82 hours				5.85 minutes	

Computations were performed on a Dell PowerEdge R510 with 2xHex-core Intel Xeon E5670 CPU processor at 2.93 GHz with 12M cache each.

Table 2. Synthetic tsunamis tested for Montauk, New York.

Scenario Name	Subduction Zone	Tsunami Source	Mw	Tsunami amplitude	
				Max (cm)	Min (cm)
ATSZAB 38-47	Atlantic	25 x (A38-47, B38-47)	9.3	53.44	-63.55
ATSZAB 48-57	Atlantic	25 x (A48-57, B48-57)	9.3	255.24	-130.60
ATSZAB 58-67	Atlantic	25 x (A58-67, B58-67)	9.3	25.76	-26.18
ATSZAB 68-77	Atlantic	25 x (A68-77, B68-77)	9.3	19.30	-17.59
ATSZAB 82-91	Atlantic	25 x (A82-91, B82-91)	9.3	49.78	-42.36
SSSZAB 01-10	South Sandwich	25 x (A01-10, B01-10)	9.3	29.49	-33.51
ATSZB52	Atlantic	1 x B52	7.5	1.41	-1.36
SSSZB11	South Sandwich	0.01 x B11	6.2	0.00	-0.00

Figure 1. Location of Montauk, New York relative to New York City.

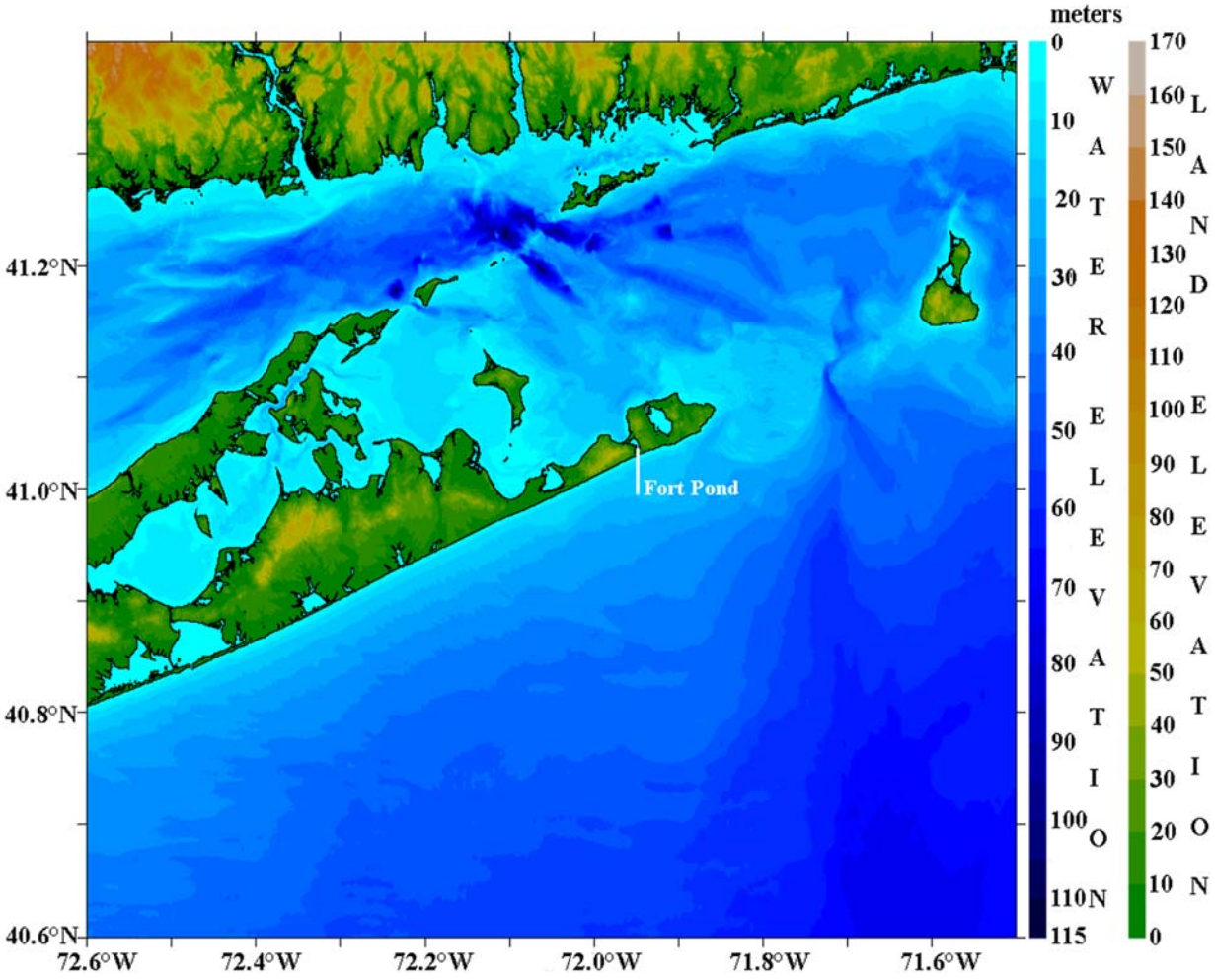

Figure 2. Extent of Digital Elevation Model (DEM) developed by NGDC (Taylor et al., 2007).

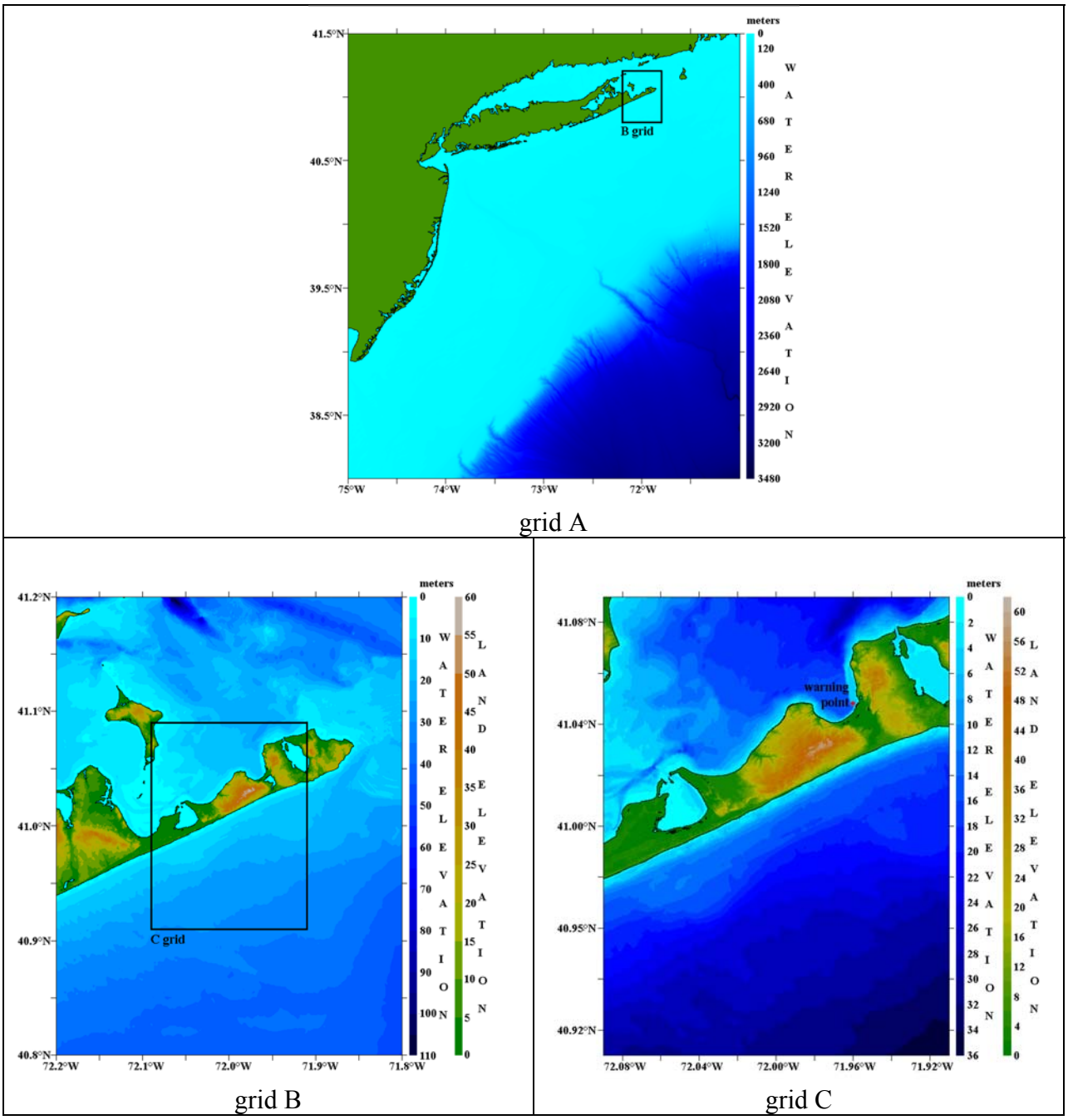

Figure 3. Extents of grids A (top), B (bottom left) and C (bottom right) for reference grid. Grid C (bottom right) red circle marks the location of the selected warning point where the Rough Rider Condominium Pier is located.

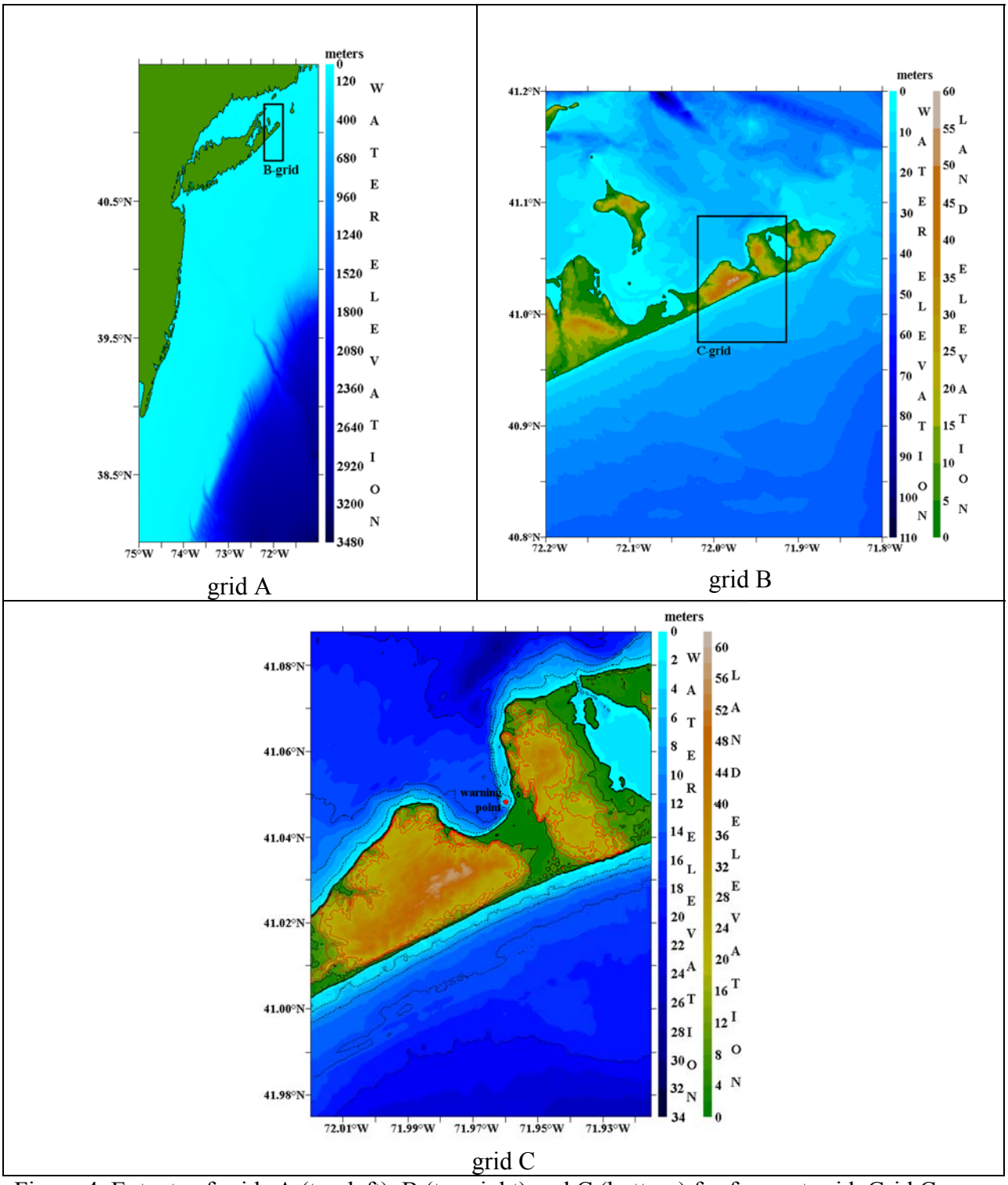

Figure 4. Extents of grids A (top left), B (top right) and C (bottom) for forecast grid. Grid C (bottom right) red circle marks the location of the selected warning point where the Rough Rider Condominium Pier is located. Water contour on grid C is from 0 to 20 m with 5 m interval. Land contour of grid C is from 0 to 5 m (black) and 10 m to 20 m with 5 m interval in red.

Figure 5. Photo of tide gauge located at the NE corner of the Rough Rider Condominium Pier.

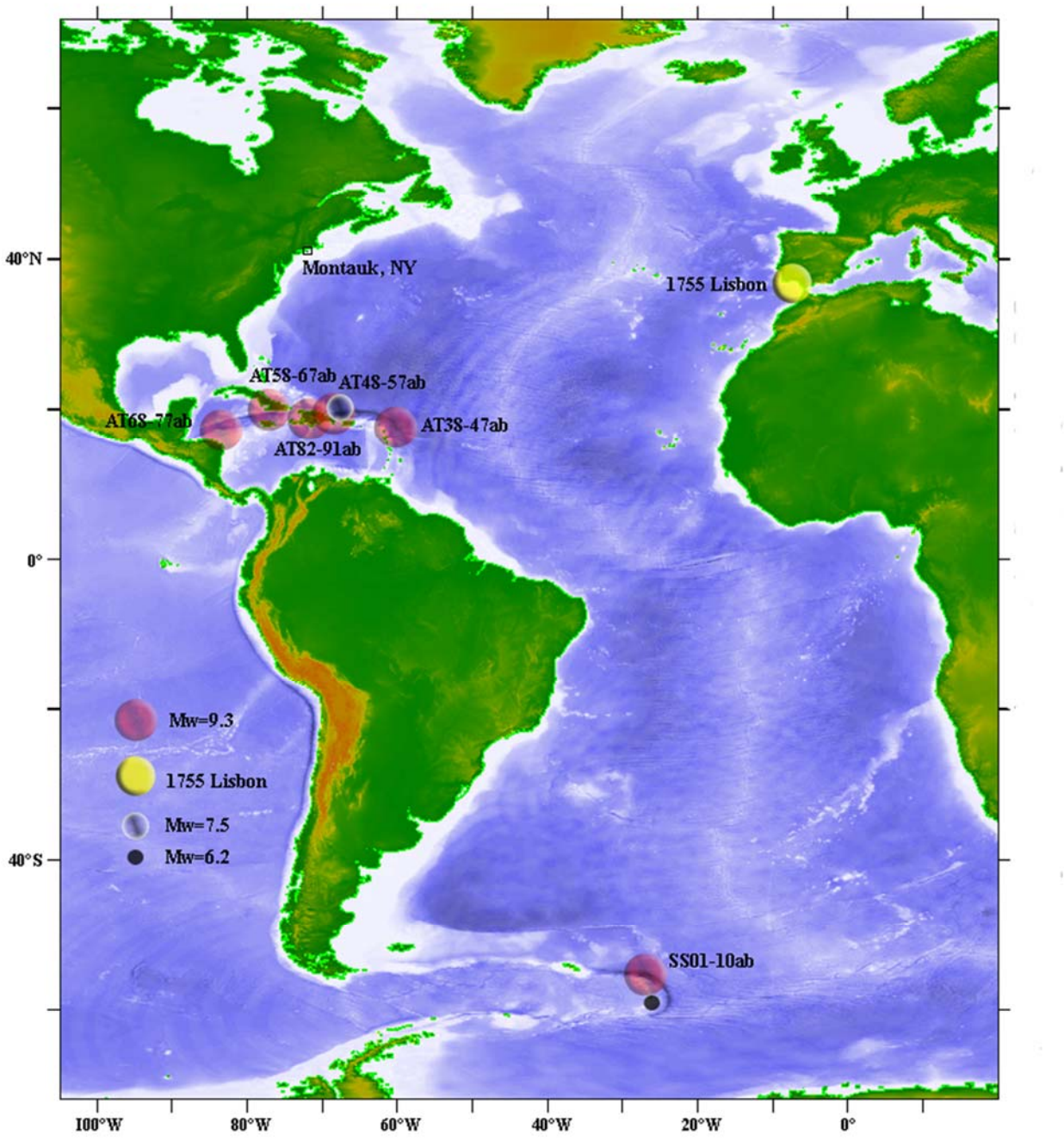

Figure 6. Location of synthetic scenarios simulated relative to Montauk.

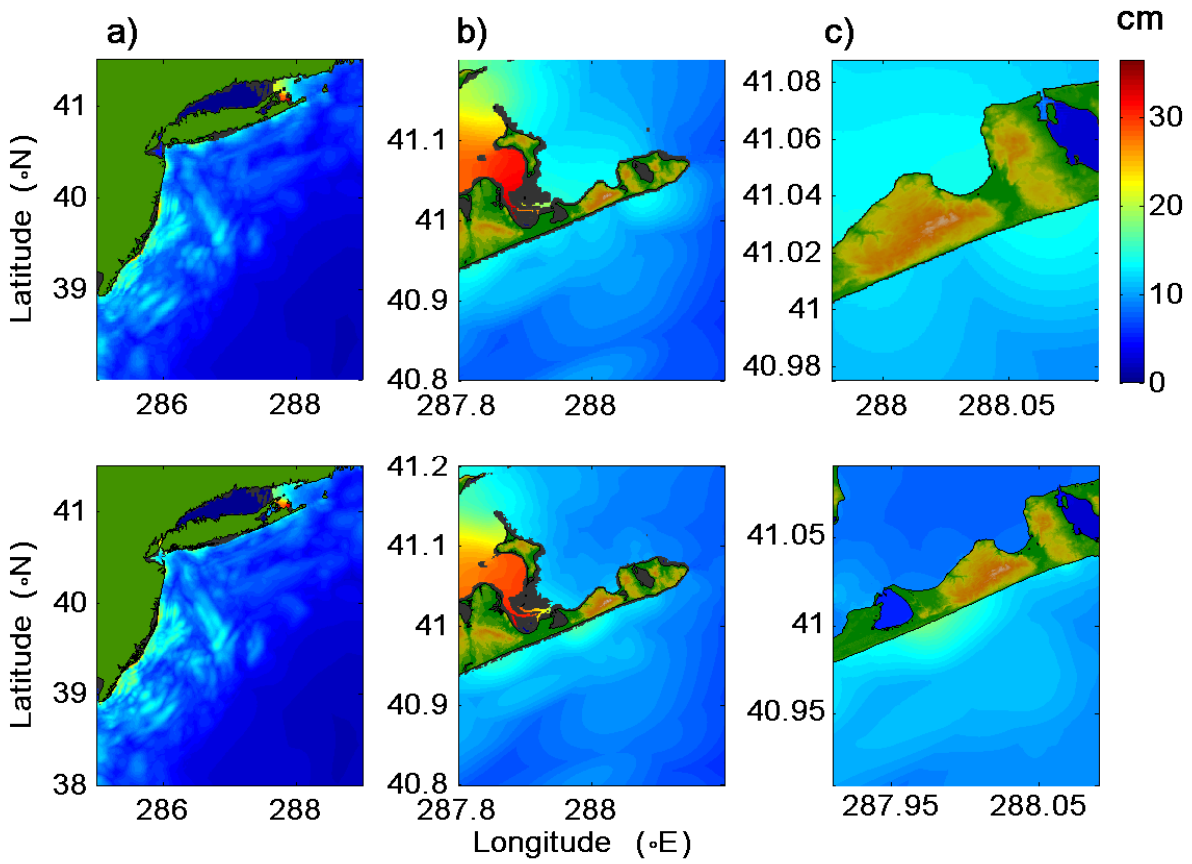

Figure 7. Maximum tsunami wave amplitude distribution for grids A, B and C (a, b and c, respectively) using 1755 Lisbon scenario. Forecast model (upper) and reference model (lower).

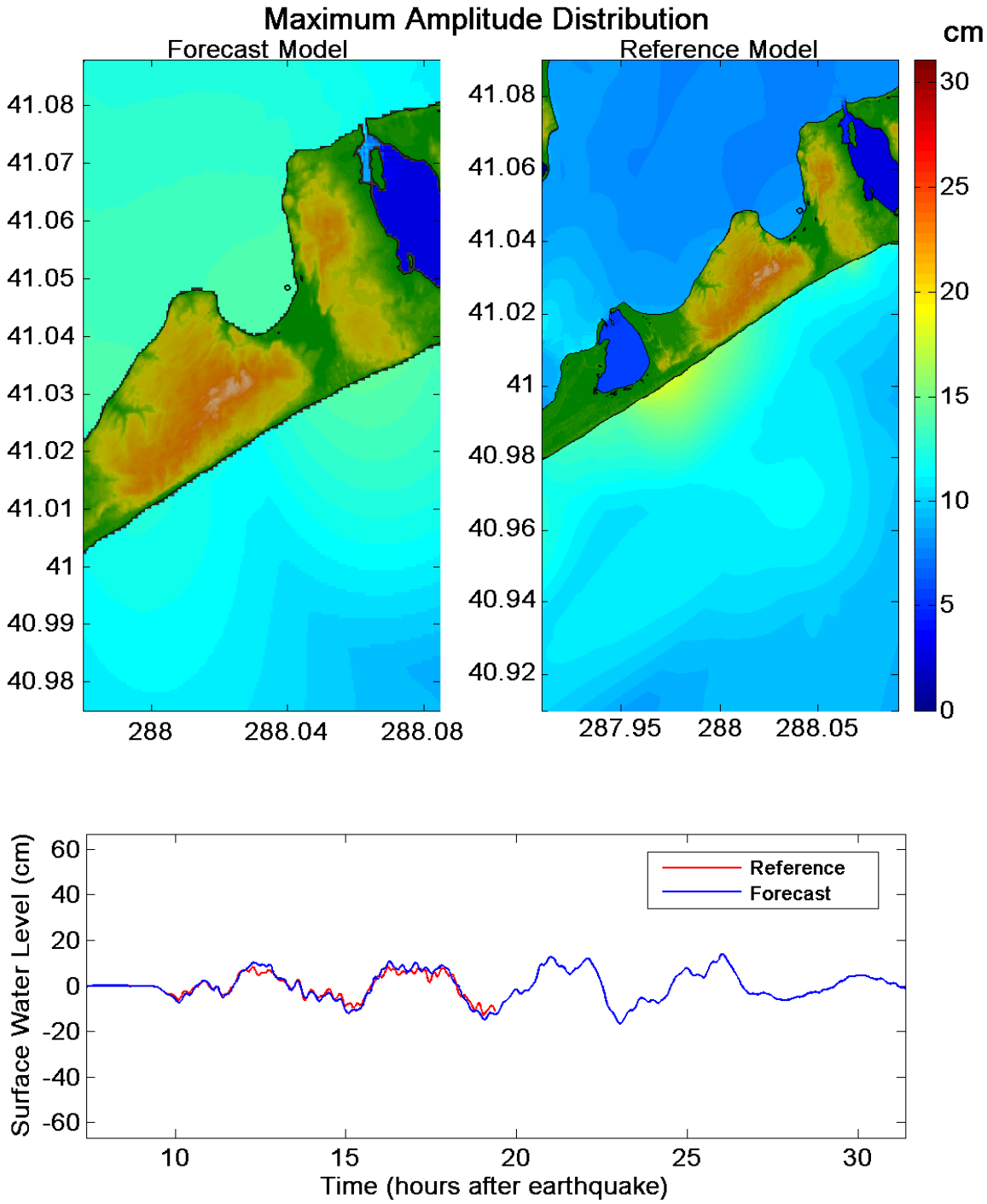

Figure 8. Maximum tsunami wave amplitude distribution of C grid for 1755 Lisbon scenario. Bottom figure is the simulated tsunami time series at the selected warning point (circle on the east side of the bay (north of Montauk)).

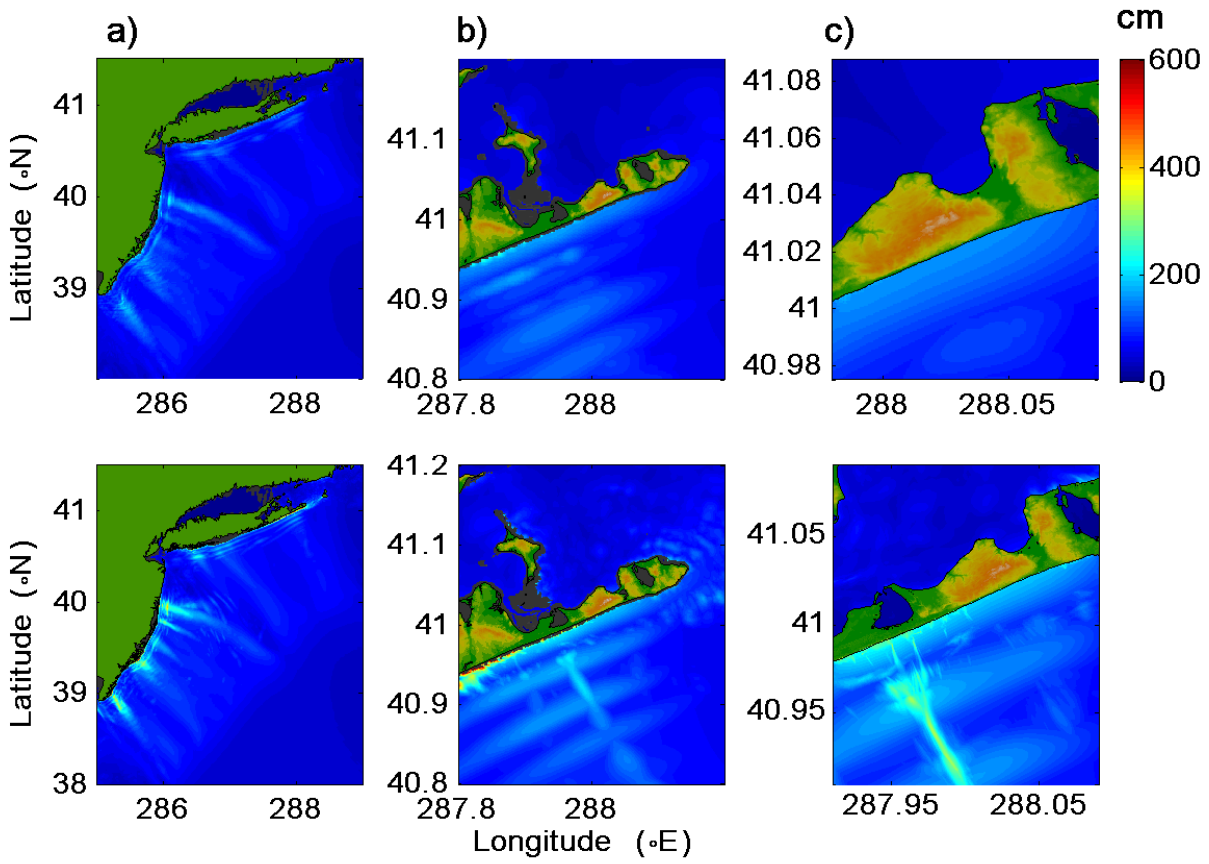

Figure 9. Maximum tsunami wave amplitude distribution for grids A, B and C (a, b and c, respectively) using synthetic scenario AT38-47ab with Mw 9.3. Forecast model (upper) and reference model (lower).

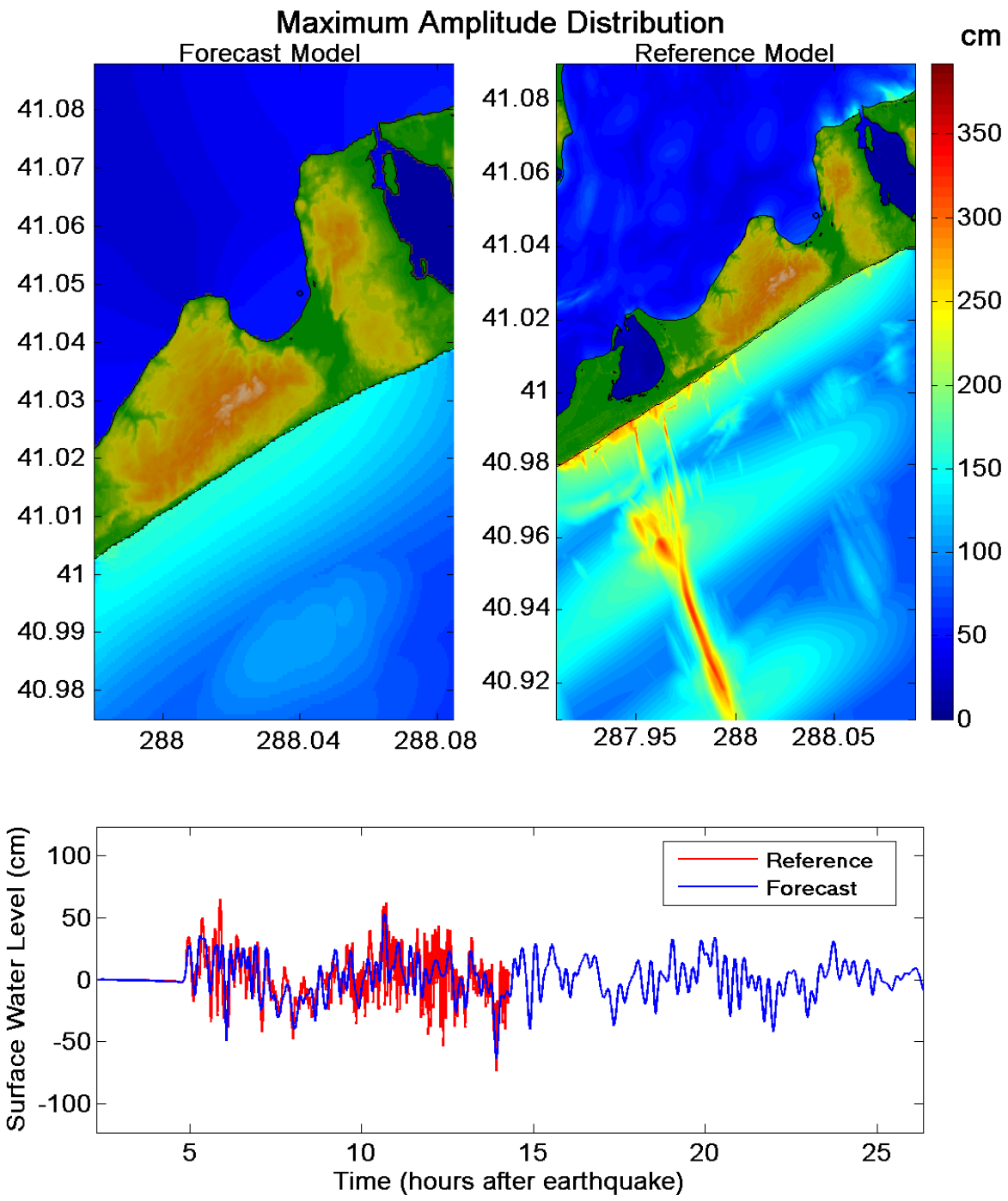

Figure 10. Maximum tsunami wave amplitude distribution of C grid for synthetic scenario AT38-47ab with Mw 9.3. Bottom figure is the simulated tsunami time series at the selected warning point (circle on the east side of the bay (north of Montauk)).

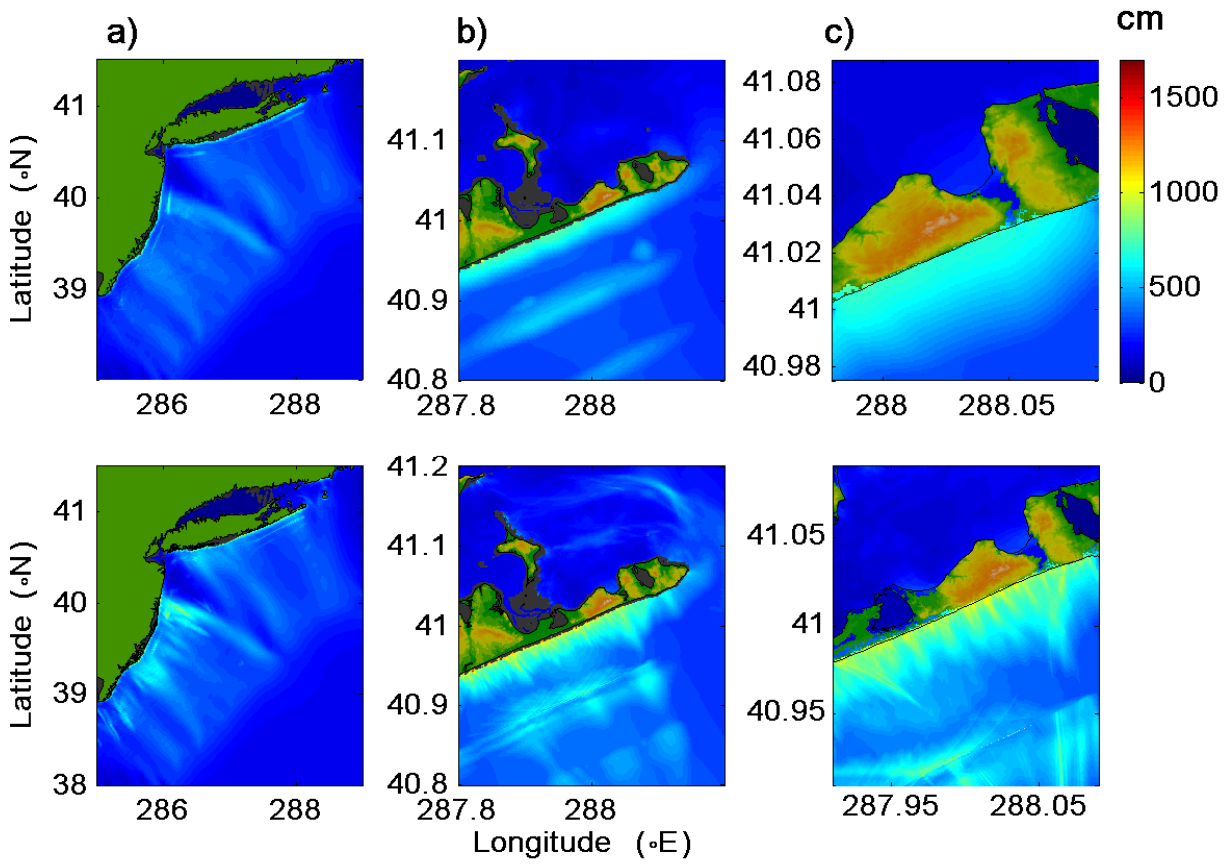

Figure 11. Maximum tsunami wave amplitude distribution for grids A, B and C (a, b and c, respectively) using synthetic scenario AT48-57ab with Mw 9.3. Forecast model (upper) and reference model (lower).

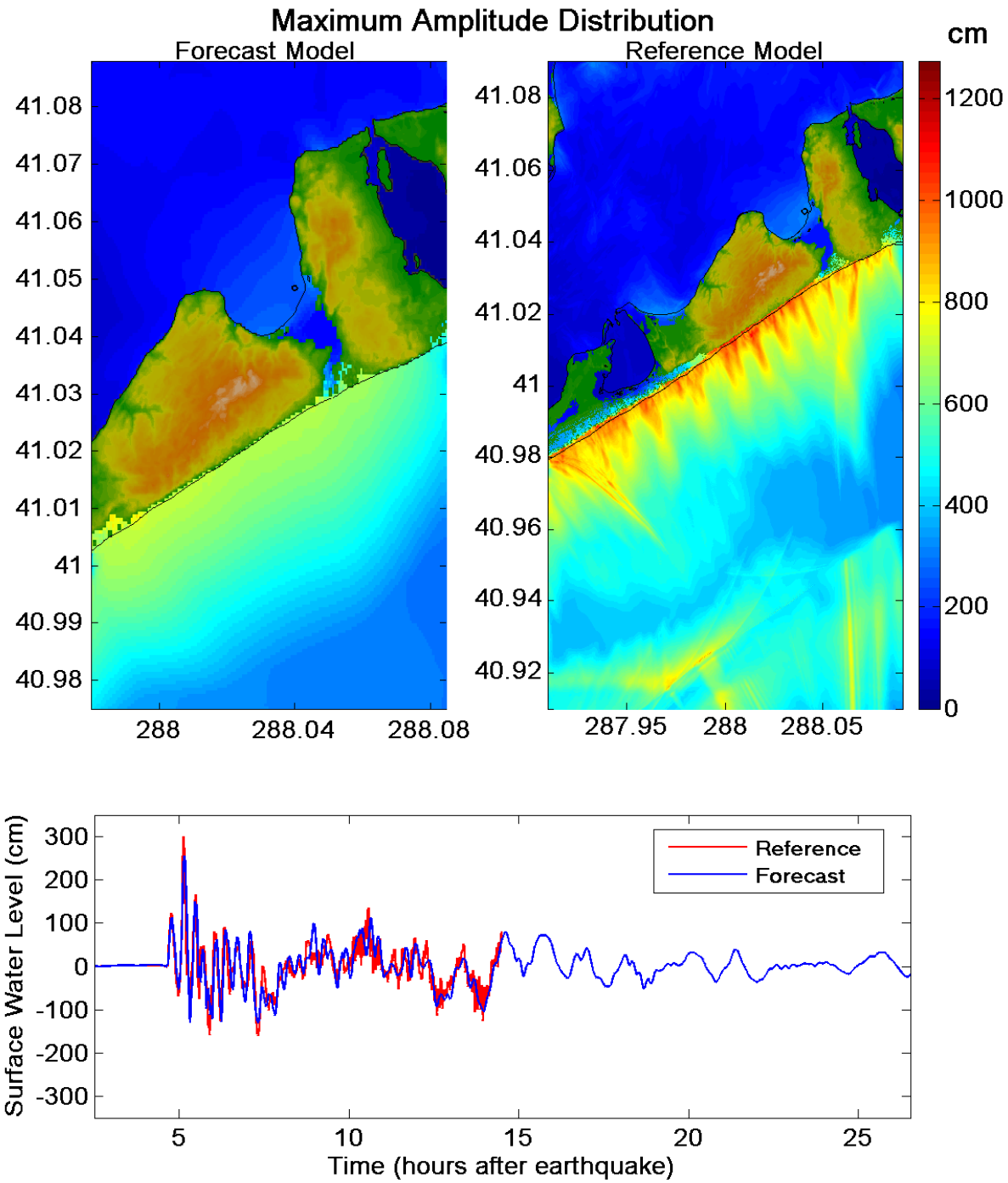

Figure 12. Maximum tsunami wave amplitude distribution of C grid for synthetic scenario AT48-57ab with Mw 9.3. Bottom figure is the simulated tsunami time series at the selected warning point (circle on the east side of the bay (north of Montauk)).

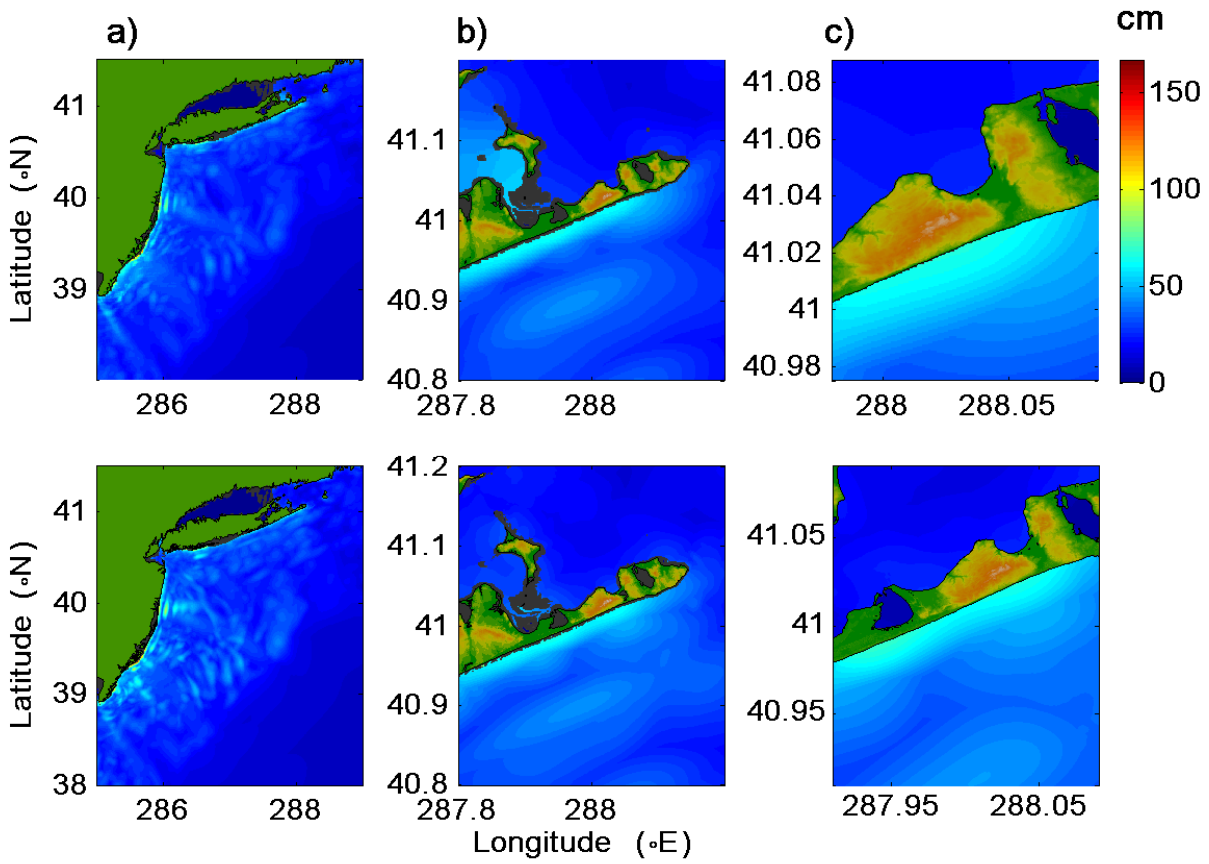

Figure 13. Maximum tsunami wave amplitude distribution for grids A, B and C (a, b and c, respectively) using synthetic scenario AT58-67ab with Mw 9.3. Forecast model (upper) and reference model (lower).

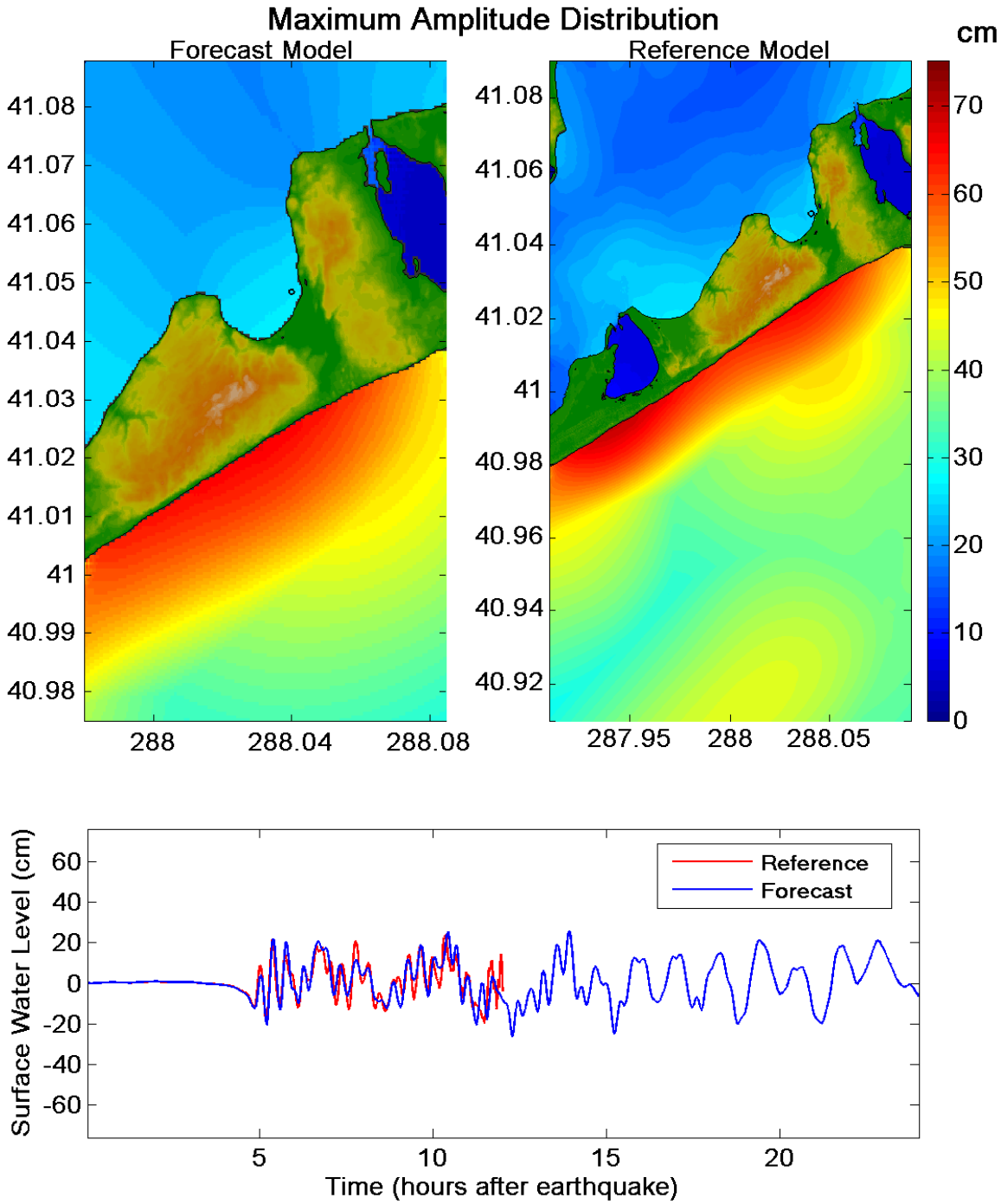

Figure 14. Maximum tsunami wave amplitude distribution of C grid for synthetic scenario AT58-67ab with Mw 9.3. Bottom figure is the simulated tsunami time series at the selected warning point (circle on the east side of the bay (north of Montauk)).

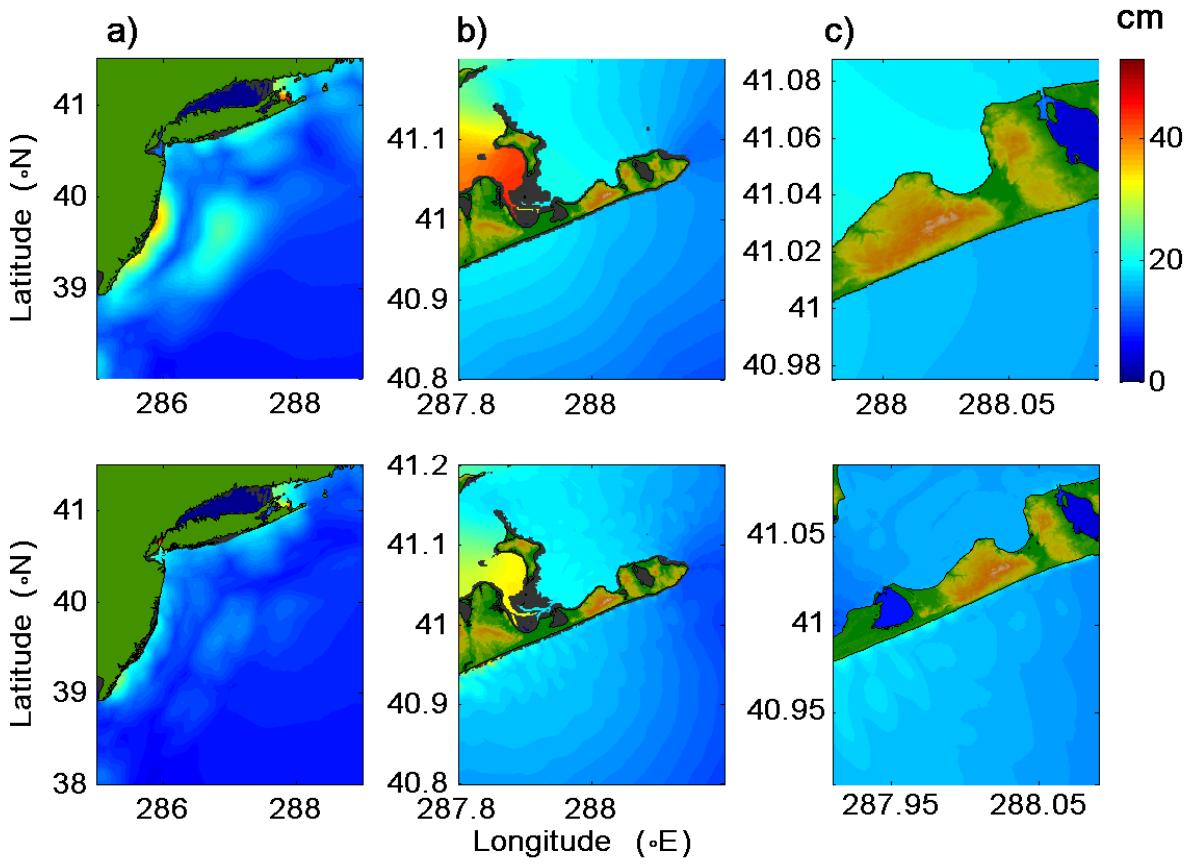

Figure 15. Maximum tsunami wave amplitude distribution for grids A, B and C (a, b and c, respectively) using synthetic scenario AT68-77ab with Mw 9.3. Forecast model (upper) and reference model (lower).

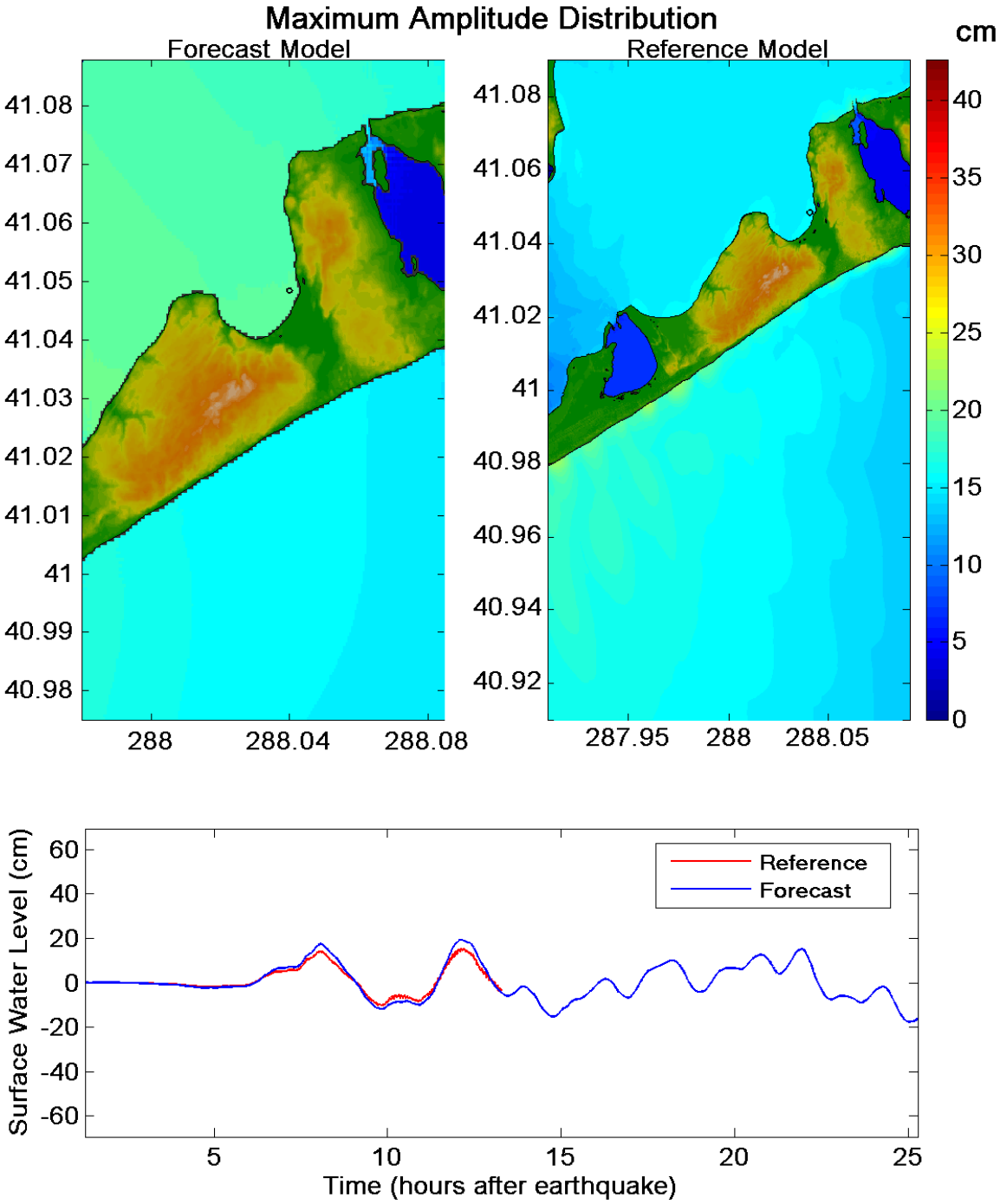

Figure 16. Maximum tsunami wave amplitude distribution of C grid for synthetic scenario AT68-77ab with Mw 9.3. Bottom figure is the simulated tsunami time series at the selected warning point (circle on the east side of the bay (north of Montauk)).

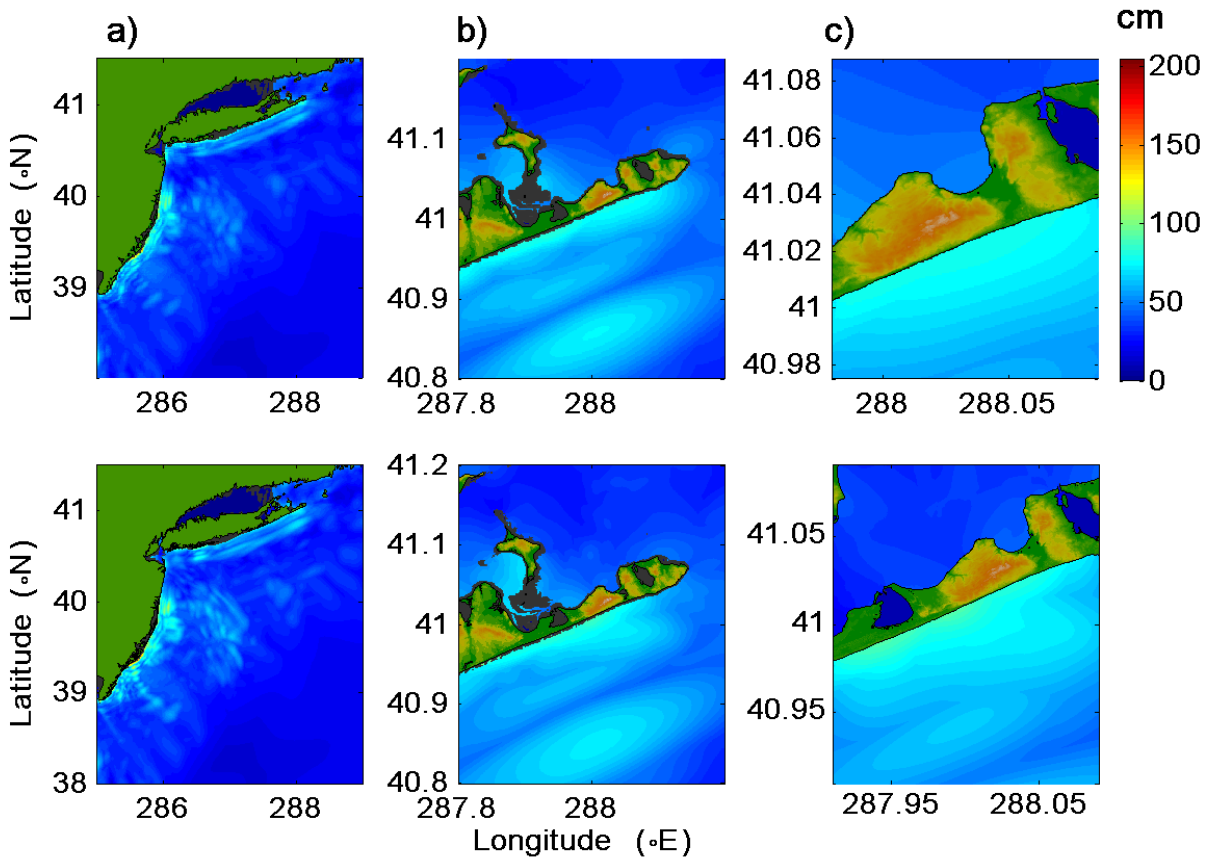

Figure 17. Maximum tsunami wave amplitude distribution for grids A, B and C (a, b and c, respectively) using synthetic scenario AT82-91ab with Mw 9.3. Forecast model (upper) and reference model (lower).

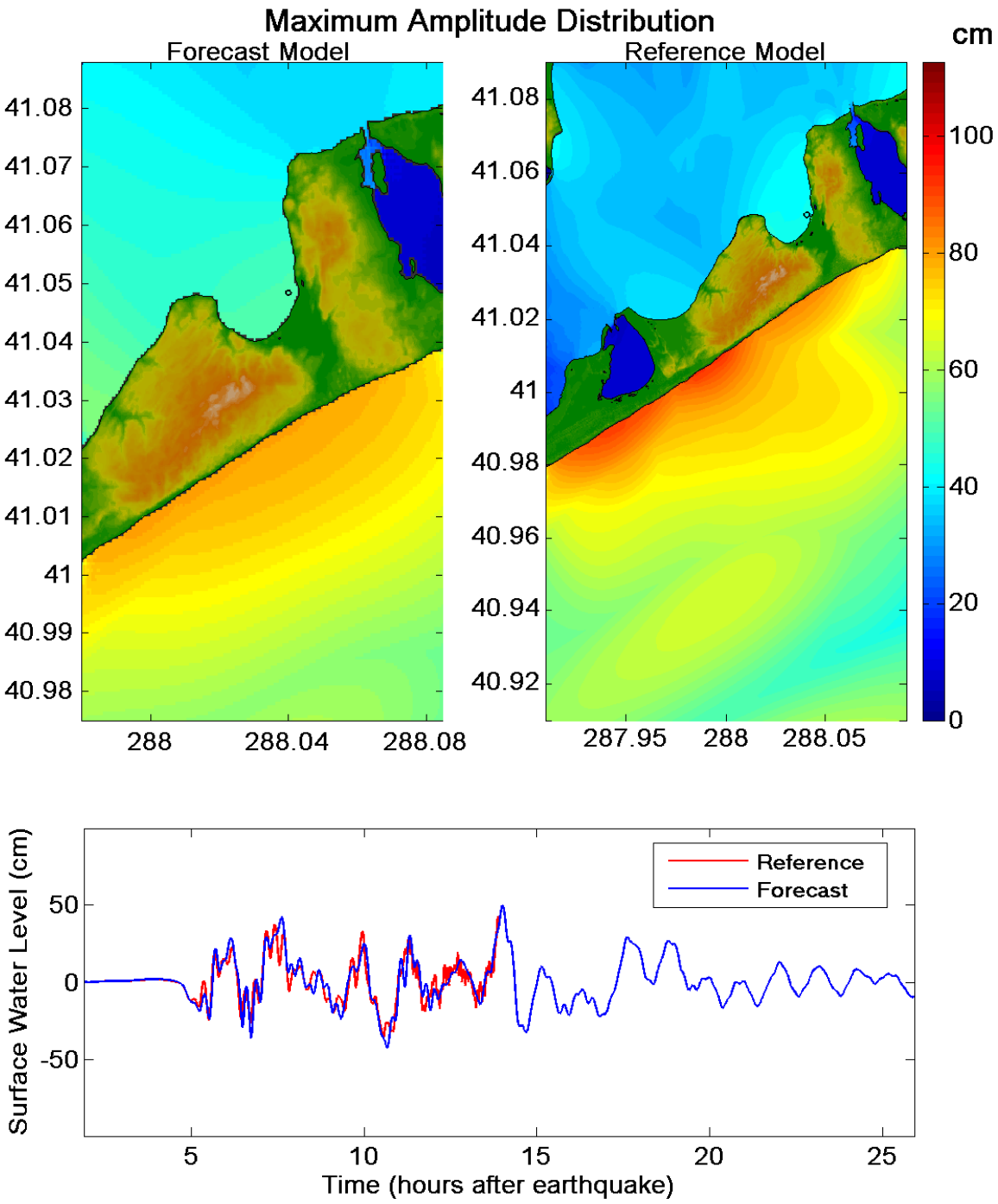

Figure 18. Maximum tsunami wave amplitude distribution of C grid for synthetic scenario AT82-91ab with Mw 9.3. Bottom figure is the simulated tsunami time series at the selected warning point (circle on the east side of the bay (north of Montauk)).

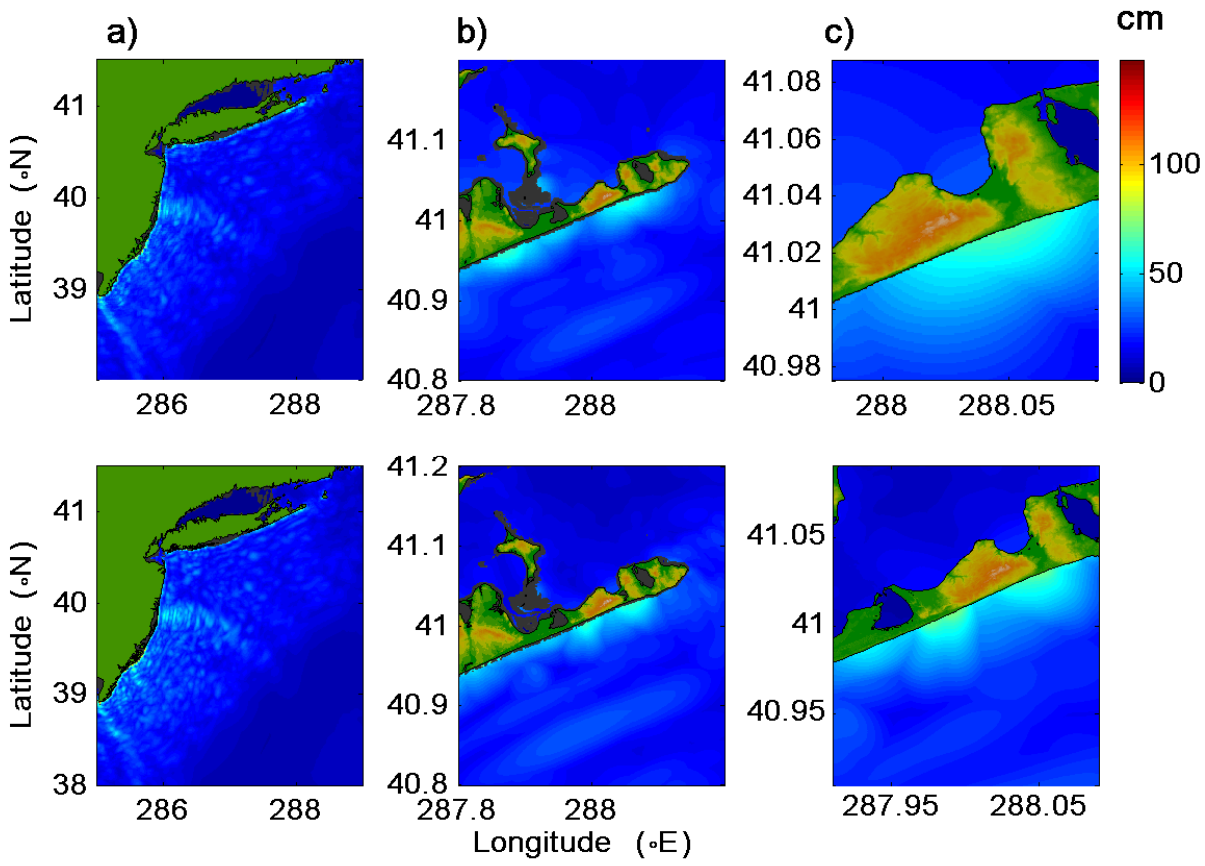

Figure 19. Maximum tsunami wave amplitude distribution for grids A, B and C (a, b and c, respectively) using synthetic scenario SS01-10ab with Mw 9.3. Forecast model (upper) and reference model (lower).

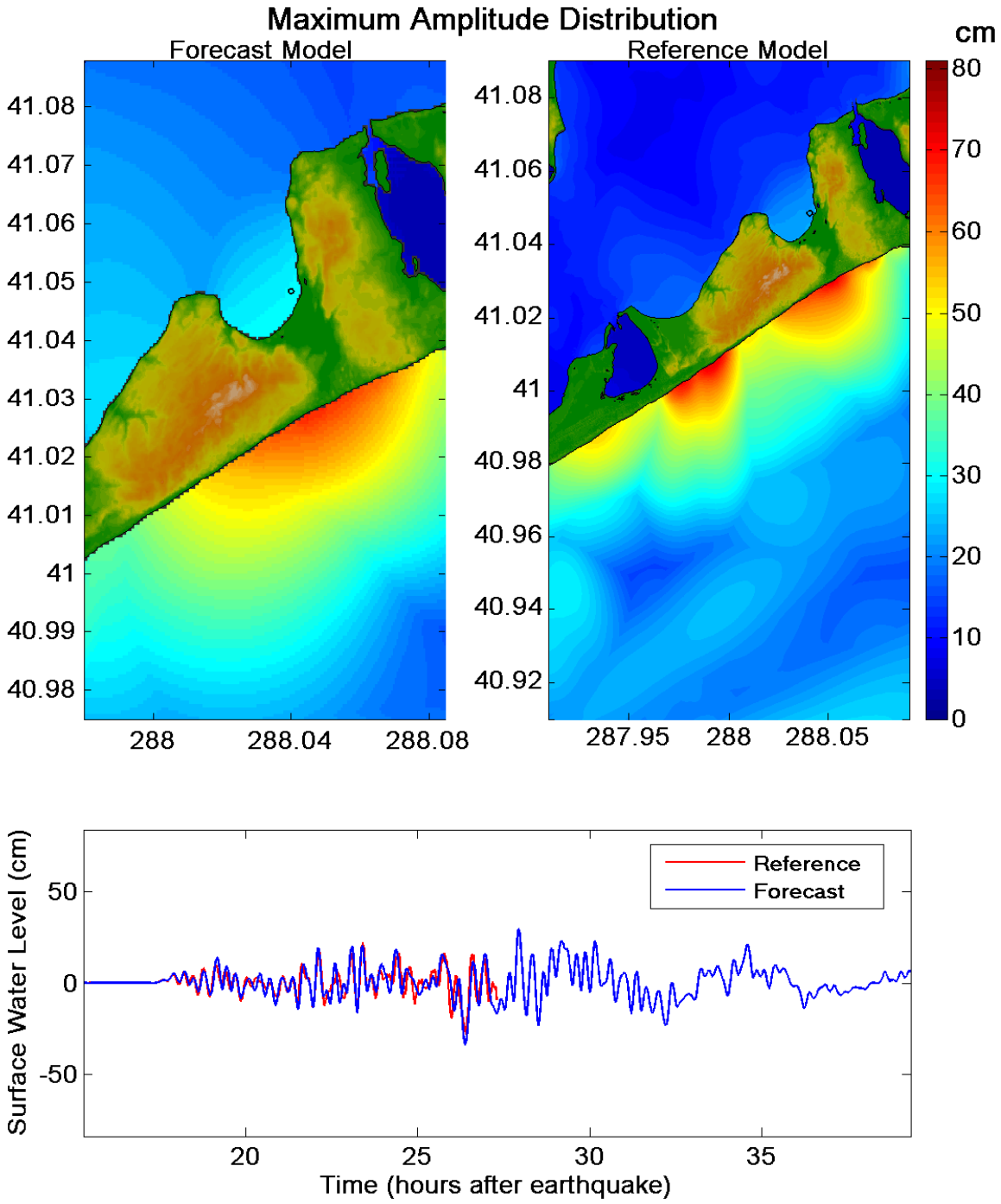

Figure 20. Maximum tsunami wave amplitude distribution of C grid for synthetic scenario SS01-10ab with Mw 9.3. Bottom figure is the simulated tsunami time series at the selected warning point (circle on the east side of the bay (north of Montauk)).

Appendix A. Most code *.in file

A1. Reference model *.in file for Montauk, New York

0.0001	Minimum amplitude of input offshore wave (m)
5	Input minimum depth for offshore (m)
0.1	Input "dry land" depth for inundation (m)
0.0009	Input friction coefficient (n**2)
1	A & B-grid runup flag (0=disallow, 1=allow runup)
200.0	Blow-up limit (maximum eta before blow-up)
0.3	Input time step (sec)
120000	Input number of steps
4	Compute "A" arrays every nth time step, n=
4	Compute "B" arrays every nth time step, n=
100	Input number of steps between snapshots
0	...Starting from
1	...Saving grid every nth node, n=1

A2. Forecast model *.in file for Montauk, New York

0.0001	Minimum amplitude of input offshore wave (m)
5	Input minimum depth for offshore (m)
0.1	Input "dry land" depth for inundation (m)
0.0009	Input friction coefficient (n**2)
1	A & B-grid runup flag (0=disallow, 1=allow runup)
300.0	Blow-up limit (maximum eta before blow-up)
2.0	Input time step (sec)
432000	Input number of steps
2	Compute "A" arrays every nth time step, n=
2	Compute "B" arrays every nth time step, n=
16	Input number of steps between snapshots
0	...Starting from
1	...Saving grid every nth node, n=1

Appendix B. Propagation Database: Atlantic Ocean Unit Sources

This section lists the earthquake parameters of each unit source in the Atlantic Ocean which covers the Caribbean and South Sandwich sources as of January 30, 2013. The development of the Montauk, New York forecast model was done March 2013.

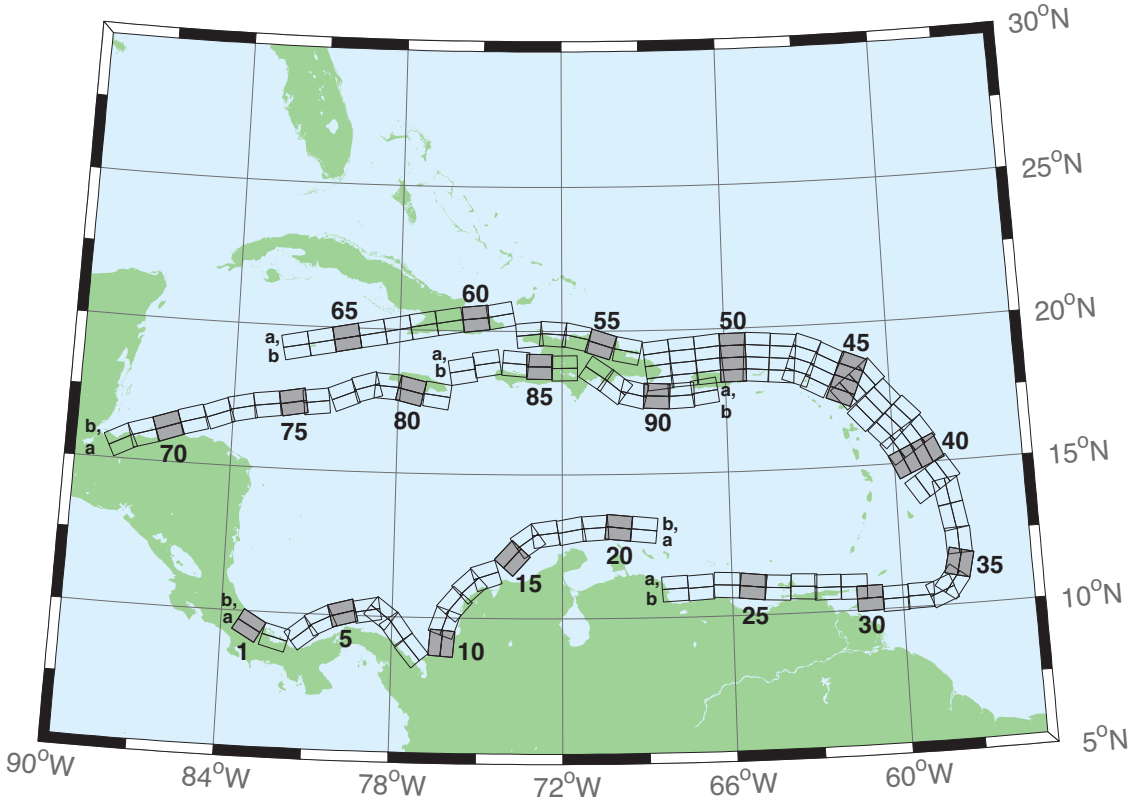

Figure B.1. Atlantic Source Zone unit sources.

Table B.1. Earthquake parameter for unit source in Atlantic.

Unit Source	Description	Lon (°)	Lat (°)	Strike (°)	Dip (°)	Depth (km)
atsz-01a	Atlantic Source Zone	-83.2020	9.1449	27.50	120.00	28.09
atsz-01b	Atlantic Source Zone	-83.0000	9.4899	27.50	120.00	5.00
atsz-02a	Atlantic Source Zone	-82.1932	8.7408	27.50	105.11	28.09
atsz-02b	Atlantic Source Zone	-82.0880	9.1254	27.50	105.11	5.00
atsz-03a	Atlantic Source Zone	-80.9172	9.0103	30.00	51.31	30.00
atsz-03b	Atlantic Source Zone	-81.1636	9.3139	30.00	51.31	5.00
atsz-04a	Atlantic Source Zone	-80.3265	9.4308	30.00	63.49	30.00
atsz-04b	Atlantic Source Zone	-80.5027	9.7789	30.00	63.49	5.00
atsz-05a	Atlantic Source Zone	-79.6247	9.6961	30.00	74.44	30.00
atsz-05b	Atlantic Source Zone	-79.7307	10.0708	30.00	74.44	5.00
atsz-06a	Atlantic Source Zone	-78.8069	9.8083	30.00	79.71	30.00
atsz-06b	Atlantic Source Zone	-78.8775	10.1910	30.00	79.71	5.00
atsz-07a	Atlantic Source Zone	-78.6237	9.7963	30.00	127.25	30.00
atsz-07b	Atlantic Source Zone	-78.3845	10.1059	30.00	127.25	5.00
atsz-08a	Atlantic Source Zone	-78.1693	9.3544	30.00	143.76	30.00
atsz-08b	Atlantic Source Zone	-77.8511	9.5844	30.00	143.76	5.00
atsz-09a	Atlantic Source Zone	-77.5913	8.5989	30.00	139.93	30.00
atsz-09b	Atlantic Source Zone	-77.2900	8.8493	30.00	139.93	5.00
atsz-10a	Atlantic Source Zone	-75.8109	9.0881	17.00	4.67	19.62
atsz-10b	Atlantic Source Zone	-76.2445	9.1231	17.00	4.67	5.00
atsz-11a	Atlantic Source Zone	-75.7406	9.6929	17.00	19.67	19.62
atsz-11b	Atlantic Source Zone	-76.1511	9.8375	17.00	19.67	5.00
atsz-12a	Atlantic Source Zone	-75.4763	10.2042	17.00	40.40	19.62
atsz-12b	Atlantic Source Zone	-75.8089	10.4826	17.00	40.40	5.00
atsz-13a	Atlantic Source Zone	-74.9914	10.7914	17.00	47.17	19.62
atsz-13b	Atlantic Source Zone	-75.2890	11.1064	17.00	47.17	5.00
atsz-14a	Atlantic Source Zone	-74.5666	11.0708	17.00	71.68	19.62
atsz-14b	Atlantic Source Zone	-74.7043	11.4786	17.00	71.68	5.00
atsz-15a	Atlantic Source Zone	-73.4576	11.8012	17.00	42.69	19.62
atsz-15b	Atlantic Source Zone	-73.7805	12.0924	17.00	42.69	5.00
atsz-16a	Atlantic Source Zone	-72.9788	12.3365	17.00	54.75	19.62
atsz-16b	Atlantic Source Zone	-73.2329	12.6873	17.00	54.75	5.00
atsz-17a	Atlantic Source Zone	-72.5454	12.5061	17.00	81.96	19.62
atsz-17b	Atlantic Source Zone	-72.6071	12.9314	17.00	81.96	5.00
atsz-18a	Atlantic Source Zone	-71.6045	12.6174	17.00	79.63	19.62
atsz-18b	Atlantic Source Zone	-71.6839	13.0399	17.00	79.63	5.00
atsz-19a	Atlantic Source Zone	-70.7970	12.7078	17.00	86.32	19.62
atsz-19b	Atlantic Source Zone	-70.8253	13.1364	17.00	86.32	5.00

Table B.1 (continued). Earthquake parameter for unit sources in Atlantic.

atsz-20a	Atlantic Source Zone	-70.0246	12.7185	17.00	95.94	19.62
atsz-20b	Atlantic Source Zone	-69.9789	13.1457	17.00	95.94	5.00
atsz-21a	Atlantic Source Zone	-69.1244	12.6320	17.00	95.94	19.62
atsz-21b	Atlantic Source Zone	-69.0788	13.0592	17.00	95.94	5.00
atsz-22a	Atlantic Source Zone	-68.0338	11.4286	15.00	266.94	17.94
atsz-22b	Atlantic Source Zone	-68.0102	10.9954	15.00	266.94	5.00
atsz-23a	Atlantic Source Zone	-67.1246	11.4487	15.00	266.94	17.94
atsz-23b	Atlantic Source Zone	-67.1010	11.0155	15.00	266.94	5.00
atsz-24a	Atlantic Source Zone	-66.1656	11.5055	15.00	273.30	17.94
atsz-24b	Atlantic Source Zone	-66.1911	11.0724	15.00	273.30	5.00
atsz-25a	Atlantic Source Zone	-65.2126	11.4246	15.00	276.36	17.94
atsz-25b	Atlantic Source Zone	-65.2616	10.9934	15.00	276.36	5.00
atsz-26a	Atlantic Source Zone	-64.3641	11.3516	15.00	272.87	17.94
atsz-26b	Atlantic Source Zone	-64.3862	10.9183	15.00	272.87	5.00
atsz-27a	Atlantic Source Zone	-63.4472	11.3516	15.00	272.93	17.94
atsz-27b	Atlantic Source Zone	-63.4698	10.9183	15.00	272.93	5.00
atsz-28a	Atlantic Source Zone	-62.6104	11.2831	15.00	271.11	17.94
atsz-28b	Atlantic Source Zone	-62.6189	10.8493	15.00	271.11	5.00
atsz-29a	Atlantic Source Zone	-61.6826	11.2518	15.00	271.57	17.94
atsz-29b	Atlantic Source Zone	-61.6947	10.8181	15.00	271.57	5.00
atsz-30a	Atlantic Source Zone	-61.1569	10.8303	15.00	269.01	17.94
atsz-30b	Atlantic Source Zone	-61.1493	10.3965	15.00	269.01	5.00
atsz-31a	Atlantic Source Zone	-60.2529	10.7739	15.00	269.01	17.94
atsz-31b	Atlantic Source Zone	-60.2453	10.3401	15.00	269.01	5.00
atsz-32a	Atlantic Source Zone	-59.3510	10.8123	15.00	269.01	17.94
atsz-32b	Atlantic Source Zone	-59.3734	10.3785	15.00	269.01	5.00
atsz-33a	Atlantic Source Zone	-58.7592	10.8785	15.00	248.62	17.94
atsz-33b	Atlantic Source Zone	-58.5984	10.4745	15.00	248.62	5.00
atsz-34a	Atlantic Source Zone	-58.5699	11.0330	15.00	217.15	17.94
atsz-34b	Atlantic Source Zone	-58.2179	10.7710	15.00	217.15	5.00
atsz-35a	Atlantic Source Zone	-58.3549	11.5300	15.00	193.68	17.94
atsz-35b	Atlantic Source Zone	-57.9248	11.4274	15.00	193.68	5.00
atsz-36a	Atlantic Source Zone	-58.3432	12.1858	15.00	177.65	17.94
atsz-36b	Atlantic Source Zone	-57.8997	12.2036	15.00	177.65	5.00
atsz-37a	Atlantic Source Zone	-58.4490	12.9725	15.00	170.73	17.94
atsz-37b	Atlantic Source Zone	-58.0095	13.0424	15.00	170.73	5.00
atsz-38a	Atlantic Source Zone	-58.6079	13.8503	15.00	170.22	17.94
atsz-38b	Atlantic Source Zone	-58.1674	13.9240	15.00	170.22	5.00
atsz-39a	Atlantic Source Zone	-58.6667	14.3915	15.00	146.85	17.94
atsz-39b	Atlantic Source Zone	-58.2913	14.6287	15.00	146.85	5.00

Table B.1 (continued). Earthquake parameter for unit sources in Atlantic.

atsz-39y	Atlantic Source Zone	-59.4168	13.9171	15.00	146.85	43.82
atsz-39z	Atlantic Source Zone	-59.0415	14.1543	15.00	146.85	30.88
atsz-40a	Atlantic Source Zone	-59.1899	15.2143	15.00	156.23	17.94
atsz-40b	Atlantic Source Zone	-58.7781	15.3892	15.00	156.23	5.00
atsz-40y	Atlantic Source Zone	-60.0131	14.8646	15.00	156.23	43.82
atsz-40z	Atlantic Source Zone	-59.6012	15.0395	15.00	156.23	30.88
atsz-41a	Atlantic Source Zone	-59.4723	15.7987	15.00	146.33	17.94
atsz-41b	Atlantic Source Zone	-59.0966	16.0392	15.00	146.33	5.00
atsz-41y	Atlantic Source Zone	-60.2229	15.3177	15.00	146.33	43.82
atsz-41z	Atlantic Source Zone	-59.8473	15.5582	15.00	146.33	30.88
atsz-42a	Atlantic Source Zone	-59.9029	16.4535	15.00	136.99	17.94
atsz-42b	Atlantic Source Zone	-59.5716	16.7494	15.00	136.99	5.00
atsz-42y	Atlantic Source Zone	-60.5645	15.8616	15.00	136.99	43.82
atsz-42z	Atlantic Source Zone	-60.2334	16.1575	15.00	136.99	30.88
atsz-43a	Atlantic Source Zone	-60.5996	17.0903	15.00	138.71	17.94
atsz-43b	Atlantic Source Zone	-60.2580	17.3766	15.00	138.71	5.00
atsz-43y	Atlantic Source Zone	-61.2818	16.5177	15.00	138.71	43.82
atsz-43z	Atlantic Source Zone	-60.9404	16.8040	15.00	138.71	30.88
atsz-44a	Atlantic Source Zone	-61.1559	17.8560	15.00	141.07	17.94
atsz-44b	Atlantic Source Zone	-60.8008	18.1286	15.00	141.07	5.00
atsz-44y	Atlantic Source Zone	-61.8651	17.3108	15.00	141.07	43.82
atsz-44z	Atlantic Source Zone	-61.5102	17.5834	15.00	141.07	30.88
atsz-45a	Atlantic Source Zone	-61.5491	18.0566	15.00	112.84	17.94
atsz-45b	Atlantic Source Zone	-61.3716	18.4564	15.00	112.84	5.00
atsz-45y	Atlantic Source Zone	-61.9037	17.2569	15.00	112.84	43.82
atsz-45z	Atlantic Source Zone	-61.7260	17.6567	15.00	112.84	30.88
atsz-46a	Atlantic Source Zone	-62.4217	18.4149	15.00	117.86	17.94
atsz-46b	Atlantic Source Zone	-62.2075	18.7985	15.00	117.86	5.00
atsz-46y	Atlantic Source Zone	-62.8493	17.6477	15.00	117.86	43.82
atsz-46z	Atlantic Source Zone	-62.6352	18.0313	15.00	117.86	30.88
atsz-47a	Atlantic Source Zone	-63.1649	18.7844	20.00	110.46	22.10
atsz-47b	Atlantic Source Zone	-63.0087	19.1798	20.00	110.46	5.00
atsz-47y	Atlantic Source Zone	-63.4770	17.9936	20.00	110.46	56.30
atsz-47z	Atlantic Source Zone	-63.3205	18.3890	20.00	110.46	39.20
atsz-48a	Atlantic Source Zone	-63.8800	18.8870	20.00	95.37	22.10
atsz-48b	Atlantic Source Zone	-63.8382	19.3072	20.00	95.37	5.00
atsz-48y	Atlantic Source Zone	-63.9643	18.0465	20.00	95.37	56.30
atsz-48z	Atlantic Source Zone	-63.9216	18.4667	20.00	95.37	39.20
atsz-49a	Atlantic Source Zone	-64.8153	18.9650	20.00	94.34	22.10
atsz-49b	Atlantic Source Zone	-64.7814	19.3859	20.00	94.34	5.00

Table B.1 (continued). Earthquake parameter for unit sources in Atlantic.

atsz-49y	Atlantic Source Zone	-64.8840	18.1233	20.00	94.34	56.30
atsz-49z	Atlantic Source Zone	-64.8492	18.5442	20.00	94.34	39.20
atsz-50a	Atlantic Source Zone	-65.6921	18.9848	20.00	89.59	22.10
atsz-50b	Atlantic Source Zone	-65.6953	19.4069	20.00	89.59	5.00
atsz-50y	Atlantic Source Zone	-65.6874	18.1407	20.00	89.59	56.30
atsz-50z	Atlantic Source Zone	-65.6887	18.5628	20.00	89.59	39.20
atsz-51a	Atlantic Source Zone	-66.5742	18.9484	20.00	84.98	22.10
atsz-51b	Atlantic Source Zone	-66.6133	19.3688	20.00	84.98	5.00
atsz-51y	Atlantic Source Zone	-66.4977	18.1076	20.00	84.98	56.30
atsz-51z	Atlantic Source Zone	-66.5353	18.5280	20.00	84.98	39.20
atsz-52a	Atlantic Source Zone	-67.5412	18.8738	20.00	85.87	22.10
atsz-52b	Atlantic Source Zone	-67.5734	19.2948	20.00	85.87	5.00
atsz-52y	Atlantic Source Zone	-67.4781	18.0319	20.00	85.87	56.30
atsz-52z	Atlantic Source Zone	-67.5090	18.4529	20.00	85.87	39.20
atsz-53a	Atlantic Source Zone	-68.4547	18.7853	20.00	83.64	22.10
atsz-53b	Atlantic Source Zone	-68.5042	19.2048	20.00	83.64	5.00
atsz-53y	Atlantic Source Zone	-68.3575	17.9463	20.00	83.64	56.30
atsz-53z	Atlantic Source Zone	-68.4055	18.3658	20.00	83.64	39.20
atsz-54a	Atlantic Source Zone	-69.6740	18.8841	20.00	101.54	22.10
atsz-54b	Atlantic Source Zone	-69.5846	19.2976	20.00	101.54	5.00
atsz-55a	Atlantic Source Zone	-70.7045	19.1376	20.00	108.19	22.10
atsz-55b	Atlantic Source Zone	-70.5647	19.5386	20.00	108.19	5.00
atsz-56a	Atlantic Source Zone	-71.5368	19.3853	20.00	102.64	22.10
atsz-56b	Atlantic Source Zone	-71.4386	19.7971	20.00	102.64	5.00
atsz-57a	Atlantic Source Zone	-72.3535	19.4838	20.00	94.20	22.10
atsz-57b	Atlantic Source Zone	-72.3206	19.9047	20.00	94.20	5.00
atsz-58a	Atlantic Source Zone	-73.1580	19.4498	20.00	84.34	22.10
atsz-58b	Atlantic Source Zone	-73.2022	19.8698	20.00	84.34	5.00
atsz-59a	Atlantic Source Zone	-74.3567	20.9620	20.00	259.74	22.10
atsz-59b	Atlantic Source Zone	-74.2764	20.5467	20.00	259.74	5.00
atsz-60a	Atlantic Source Zone	-75.2386	20.8622	15.00	264.18	17.94
atsz-60b	Atlantic Source Zone	-75.1917	20.4306	15.00	264.18	5.00
atsz-61a	Atlantic Source Zone	-76.2383	20.7425	15.00	260.70	17.94
atsz-61b	Atlantic Source Zone	-76.1635	20.3144	15.00	260.70	5.00
atsz-62a	Atlantic Source Zone	-77.2021	20.5910	15.00	259.95	17.94
atsz-62b	Atlantic Source Zone	-77.1214	20.1638	15.00	259.95	5.00
atsz-63a	Atlantic Source Zone	-78.1540	20.4189	15.00	259.03	17.94
atsz-63b	Atlantic Source Zone	-78.0661	19.9930	15.00	259.03	5.00
atsz-64a	Atlantic Source Zone	-79.0959	20.2498	15.00	259.24	17.94
atsz-64b	Atlantic Source Zone	-79.0098	19.8236	15.00	259.24	5.00

Table B.1 (continued). Earthquake parameter for unit sources in Atlantic.

atsz-65a	Atlantic Source Zone	-80.0393	20.0773	15.00	258.85	17.94
atsz-65b	Atlantic Source Zone	-79.9502	19.6516	15.00	258.85	5.00
atsz-66a	Atlantic Source Zone	-80.9675	19.8993	15.00	258.60	17.94
atsz-66b	Atlantic Source Zone	-80.8766	19.4740	15.00	258.60	5.00
atsz-67a	Atlantic Source Zone	-81.9065	19.7214	15.00	258.51	17.94
atsz-67b	Atlantic Source Zone	-81.8149	19.2962	15.00	258.51	5.00
atsz-68a	Atlantic Source Zone	-87.8003	15.2509	15.00	62.69	17.94
atsz-68b	Atlantic Source Zone	-88.0070	15.6364	15.00	62.69	5.00
atsz-69a	Atlantic Source Zone	-87.0824	15.5331	15.00	72.73	17.94
atsz-69b	Atlantic Source Zone	-87.2163	15.9474	15.00	72.73	5.00
atsz-70a	Atlantic Source Zone	-86.1622	15.8274	15.00	70.64	17.94
atsz-70b	Atlantic Source Zone	-86.3120	16.2367	15.00	70.64	5.00
atsz-71a	Atlantic Source Zone	-85.3117	16.1052	15.00	73.70	17.94
atsz-71b	Atlantic Source Zone	-85.4387	16.5216	15.00	73.70	5.00
atsz-72a	Atlantic Source Zone	-84.3470	16.3820	15.00	69.66	17.94
atsz-72b	Atlantic Source Zone	-84.5045	16.7888	15.00	69.66	5.00
atsz-73a	Atlantic Source Zone	-83.5657	16.6196	15.00	77.36	17.94
atsz-73b	Atlantic Source Zone	-83.6650	17.0429	15.00	77.36	5.00
atsz-74a	Atlantic Source Zone	-82.7104	16.7695	15.00	82.35	17.94
atsz-74b	Atlantic Source Zone	-82.7709	17.1995	15.00	82.35	5.00
atsz-75a	Atlantic Source Zone	-81.7297	16.9003	15.00	79.86	17.94
atsz-75b	Atlantic Source Zone	-81.8097	17.3274	15.00	79.86	5.00
atsz-76a	Atlantic Source Zone	-80.9196	16.9495	15.00	82.95	17.94
atsz-76b	Atlantic Source Zone	-80.9754	17.3801	15.00	82.95	5.00
atsz-77a	Atlantic Source Zone	-79.8086	17.2357	15.00	67.95	17.94
atsz-77b	Atlantic Source Zone	-79.9795	17.6378	15.00	67.95	5.00
atsz-78a	Atlantic Source Zone	-79.0245	17.5415	15.00	73.61	17.94
atsz-78b	Atlantic Source Zone	-79.1532	17.9577	15.00	73.61	5.00
atsz-79a	Atlantic Source Zone	-78.4122	17.5689	15.00	94.07	17.94
atsz-79b	Atlantic Source Zone	-78.3798	18.0017	15.00	94.07	5.00
atsz-80a	Atlantic Source Zone	-77.6403	17.4391	15.00	103.33	17.94
atsz-80b	Atlantic Source Zone	-77.5352	17.8613	15.00	103.33	5.00
atsz-81a	Atlantic Source Zone	-76.6376	17.2984	15.00	98.21	17.94
atsz-81b	Atlantic Source Zone	-76.5726	17.7278	15.00	98.21	5.00
atsz-82a	Atlantic Source Zone	-75.7299	19.0217	15.00	260.15	17.94
atsz-82b	Atlantic Source Zone	-75.6516	18.5942	15.00	260.15	5.00
atsz-83a	Atlantic Source Zone	-74.8351	19.2911	15.00	260.83	17.94
atsz-83b	Atlantic Source Zone	-74.7621	18.8628	15.00	260.83	5.00
atsz-84a	Atlantic Source Zone	-73.6639	19.2991	15.00	274.84	17.94
atsz-84b	Atlantic Source Zone	-73.7026	18.8668	15.00	274.84	5.00

Table B.1 (continued). Earthquake parameter for unit sources in Atlantic.

atsz-85a	Atlantic Source Zone	-72.8198	19.2019	15.00	270.60	17.94
atsz-85b	Atlantic Source Zone	-72.8246	18.7681	15.00	270.60	5.00
atsz-86a	Atlantic Source Zone	-71.9143	19.1477	15.00	269.06	17.94
atsz-86b	Atlantic Source Zone	-71.9068	18.7139	15.00	269.06	5.00
atsz-87a	Atlantic Source Zone	-70.4738	18.8821	15.00	304.49	17.94
atsz-87b	Atlantic Source Zone	-70.7329	18.5245	15.00	304.49	5.00
atsz-88a	Atlantic Source Zone	-69.7710	18.3902	15.00	308.94	17.94
atsz-88b	Atlantic Source Zone	-70.0547	18.0504	15.00	308.44	5.00
atsz-89a	Atlantic Source Zone	-69.2635	18.2099	15.00	283.88	17.94
atsz-89b	Atlantic Source Zone	-69.3728	17.7887	15.00	283.88	5.00
atsz-90a	Atlantic Source Zone	-68.5059	18.1443	15.00	272.93	17.94
atsz-90b	Atlantic Source Zone	-68.5284	17.7110	15.00	272.93	5.00
atsz-91a	Atlantic Source Zone	-67.6428	18.1438	15.00	267.84	17.94
atsz-91b	Atlantic Source Zone	-67.6256	17.7103	15.00	267.84	5.00
atsz-92a	Atlantic Source Zone	-66.8261	18.2536	15.00	262.00	17.94
atsz-92b	Atlantic Source Zone	-66.7627	17.8240	15.00	262.00	5.00

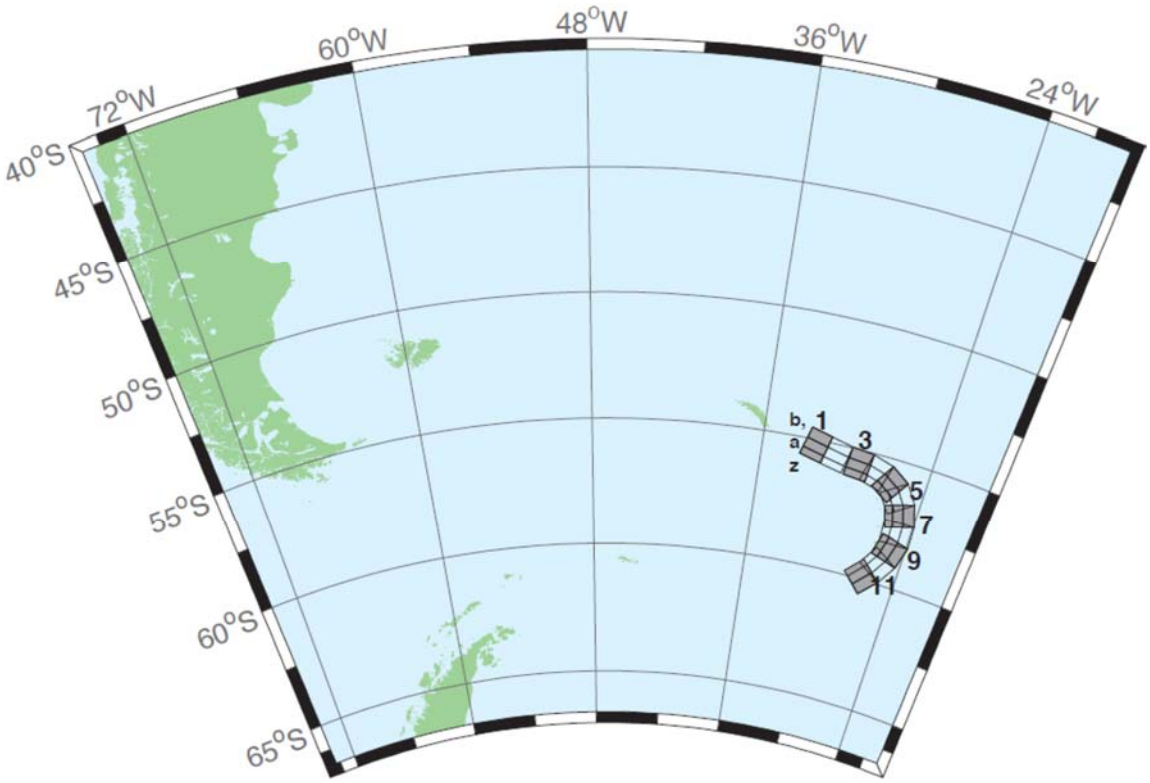

Figure B.2. South Sandwich source zone unit sources.

Table B.2. Earthquake parameters for unit sources in South Sandwich source zone.

sssz-01a	South Sandwich Source Zone	-32.3713	-55.4655	28.528	104.6905	17.511
sssz-01b	South Sandwich Source Zone	-32.1953	-55.0832	9.957	104.6905	8.866
sssz-01z	South Sandwich Source Zone	-32.5091	-55.7624	46.989	104.6905	41.391
sssz-2a	South Sandwich Source Zone	-30.8028	-55.6842	28.528	102.4495	17.511
sssz-02b	South Sandwich Source Zone	-30.6524	-55.2982	9.957	102.4495	8.866
sssz-02z	South Sandwich Source Zone	-30.9207	-55.9839	46.989	102.4495	41.391
sssz-03a	South Sandwich Source Zone	-29.0824	-55.8403	28.528	95.5322	17.511
sssz-03b	South Sandwich Source Zone	-29.0149	-55.4469	9.957	95.5322	8.866
sssz-03z	South Sandwich Source Zone	-29.1354	-56.1458	46.989	95.5322	41.391
sssz-04a	South Sandwich Source Zone	-27.8128	-55.9796	28.528	106.1387	17.511
sssz-04b	South Sandwich Source Zone	-27.6174	-55.5999	9.957	106.1387	8.866
sssz-04z	South Sandwich Source Zone	-27.9659	-56.2744	46.989	106.1387	41.391
sssz-05a	South Sandwich Source Zone	-26.7928	-56.2481	28.528	123.1030	17.511
sssz-05b	South Sandwich Source Zone	-26.4059	-55.9170	9.957	123.1030	8.866
sssz-05z	South Sandwich Source Zone	-27.0955	-56.5052	46.989	123.1030	41.391
sssz-06a	South Sandwich Source Zone	-26.1317	-56.6466	23.277	145.6243	16.110
sssz-06b	South Sandwich Source Zone	-25.5131	-56.4133	9.090	145.6243	8.228
sssz-06z	South Sandwich Source Zone	-26.5920	-56.8194	47.151	145.6243	35.869
sssz-07a	South Sandwich Source Zone	-25.6787	-57.2162	21.210	162.9420	14.235
sssz-07b	South Sandwich Source Zone	-24.9394	-57.0932	7.596	162.9420	7.626
sssz-07z	South Sandwich Source Zone	-26.2493	-57.3109	44.159	162.9420	32.324
sssz-08a	South Sandwich Source Zone	-25.5161	-57.8712	20.328	178.2111	15.908
sssz-08b	South Sandwich Source Zone	-24.7233	-57.8580	8.449	178.2111	8.562
sssz-08z	South Sandwich Source Zone	-26.1280	-57.8813	43.649	178.2111	33.278
sssz-09a	South Sandwich Source Zone	-25.6657	-58.5053	25.759	195.3813	15.715
sssz-09b	South Sandwich Source Zone	-24.9168	-58.6128	8.254	195.3813	8.537
sssz-09z	South Sandwich Source Zone	-26.1799	-58.4313	51.691	195.3813	37.444
sssz-10a	South Sandwich Source Zone	-26.1563	-59.1048	32.821	212.5129	15.649
sssz-10b	South Sandwich Source Zone	-25.5335	-59.3080	10.449	212.5129	6.581
sssz-10z	South Sandwich Source Zone	-26.5817	-58.9653	54.773	212.5129	42.750
sssz-11a	South Sandwich Source Zone	-27.0794	-59.6799	33.667	224.2397	15.746
sssz-11b	South Sandwich Source Zone	-26.5460	-59.9412	11.325	224.2397	5.927
sssz-11z	South Sandwich Source Zone	-27.4245	-59.5098	57.190	224.2397	43.464

Appendix C. Forecast Model test in SIFT system.

Forecast models are tested with synthetic tsunami events covering a range of tsunami source locations and magnitudes. Testing is also done with selected historical tsunami events when available.

The purpose of forecast model testing is three-fold. The first objective is to assure that the results obtained with the NOAA's tsunami forecast system software, which has been released to the Tsunami Warning Centers for operational use, are consistent with those obtained by the researcher during the development of the forecast model. The second objective is to test the forecast model for consistency, accuracy, time efficiency, and quality of results over a range of possible tsunami locations and magnitudes. The third objective is to identify bugs and issues in need of resolution by the researcher who developed the Forecast Model or by the forecast system software development team before the next version release to NOAA's two Tsunami Warning Centers.

Local hardware and software applications, and tools familiar to the researcher(s), are used to run the Method of Splitting Tsunamis (MOST) model during the forecast model development. The test results presented in this report lend confidence that the model performs as developed and produces the same results when initiated within the forecast system application in an operational setting as those produced by the researcher during the forecast model development. The test results assure those who rely on the Montauk, New York tsunami forecast model that consistent results are produced irrespective of system.

C.1 Test Procedure

The general procedure for forecast model testing is to run a set of synthetic tsunami scenarios and a selected set of historical tsunami events through the forecast system application and compare the results with those obtained by the researcher during the forecast model development and presented in the Tsunami Forecast Model Report. Specific steps taken to test the model include:

1. Identification of testing scenarios, including the standard set of synthetic events, appropriate historical events, and customized synthetic scenarios that may have been used by the researcher(s) in developing the forecast model.
2. Creation of new events to represent customized synthetic scenarios used by the researcher(s) in developing the forecast model, if any.
3. Submission of test model runs with the forecast system, and export of the results from A, B, and C grids, along with time series.
4. Recording applicable metadata, including the specific forecast system version used for testing.
5. Examination of forecast model results for instabilities in both time series and plot results.
6. Comparison of forecast model results obtained through the forecast system with those obtained during the forecast model development.
7. Summarization of results with specific mention of quality, consistency, and time efficiency.
8. Reporting of issues identified to modeler and forecast system software development team.

9. Retesting the forecast models in the forecast system when reported issues have been addressed or explained.

Synthetic model runs were tested on a DELL PowerEdge R510 computer equipped with two Xeon E5670 processors at 2.93 GHz, each with 12 MBytes of cache and 32GB memory. The processors are hex core and support hyper-threading, resulting in the computer performing as a 24 processor core machine. Additionally, the testing computer supports 10 Gigabit Ethernet for fast network connections. This computer configuration is similar or the same as the configurations of the computers installed at the Tsunami Warning Centers so the compute times should only vary slightly.

C.2 Results

The Montauk forecast model was tested with SIFT version 3.2.

The Montauk, New York forecast model was tested with three synthetic scenarios. Test results from the forecast system and comparisons with the results obtained during the forecast model development are shown numerically in Table C.1 and graphically in Figures C.1 to C.3. The results show that the minimum and maximum amplitudes and time series obtained from the forecast system agree with those obtained during the forecast model development, and that the forecast model is stable and robust, with consistent and high quality results across geographically distributed tsunami sources. The model run time (wall clock time) was less than 15.1 minutes for 12 hours of simulation time, and 5 minutes for 4.0 hours. This run time is within the 10 minute run time for 4 hours of simulation time and satisfies run time requirements.

A suite of three synthetic events was run on the Montauk forecast model. The modeled scenarios were stable for all cases run with no inconsistencies or ringing. The largest modeled height was 255 centimeters (cm) from the Atlantic (ATSZ 48-57) source zone. The smallest signal of 20 cm was recorded at the far field South Sandwich (SSSZ 1-10) source zone. It should be noted that the largest and smallest signal indicated is only based on the three synthetic scenarios tested in SIFT. The maximum value for this case in Table 1 differs because during development, the model was run for a longer period of time and recorded a higher value at a later hour. Maximum and minimum values and visual comparisons between the development cases and the forecast system output were consistent in shape and amplitude for both of the Atlantic cases run. The Montauk reference point used for the forecast model development is the same as what is deployed in the forecast system, so the results can be considered valid for the three cases studied.

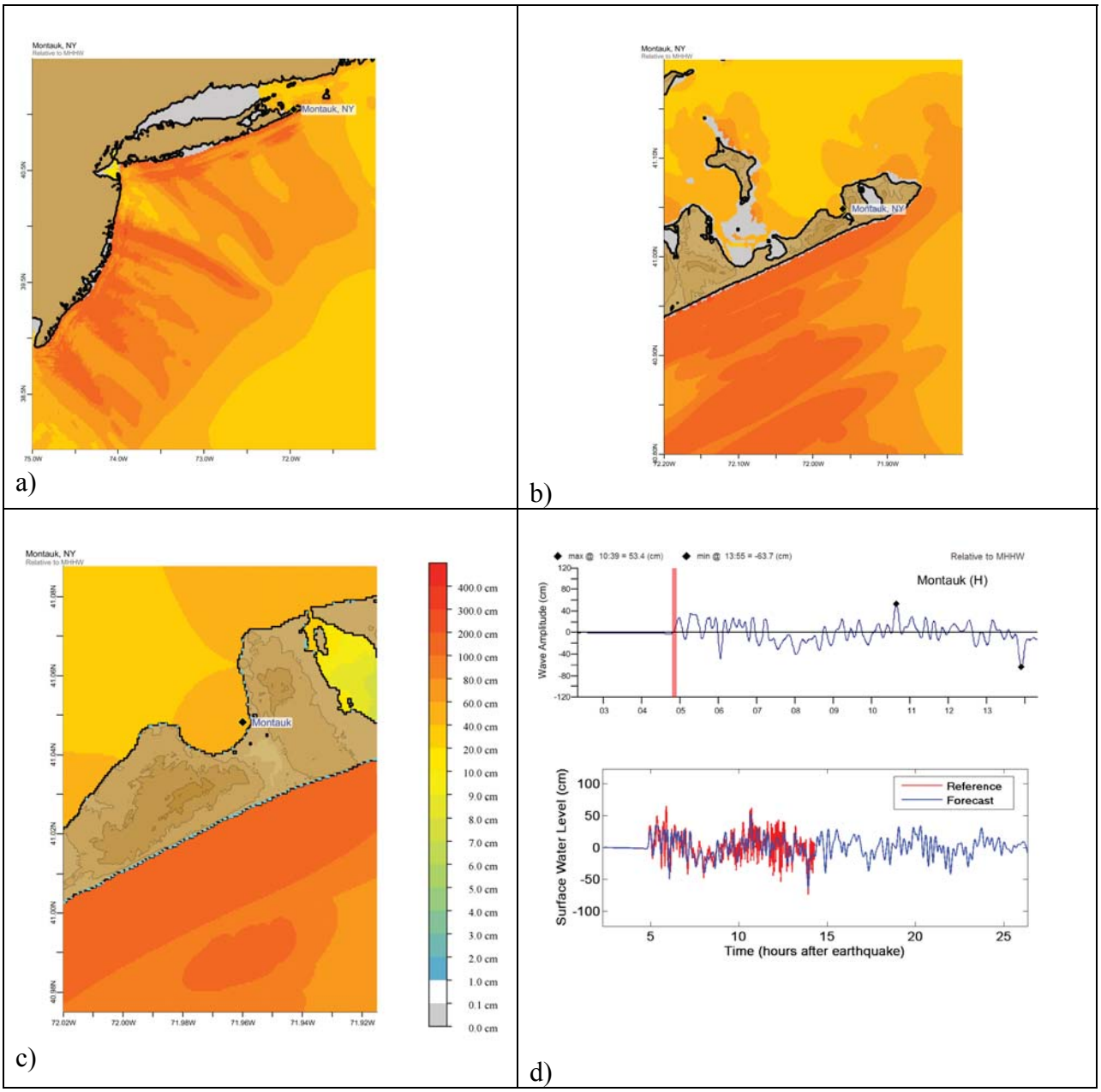

Figure C.1. Response of the Montauk forecast model to synthetic scenario ATSZ 38-47 (alpha=25). Maximum sea surface elevation for (a) A grid, b) B grid, c) C grid. Sea surface elevation time series at the C grid warning point (d). The lower time series plot is the result obtained during model development and is shown for comparison with test results.

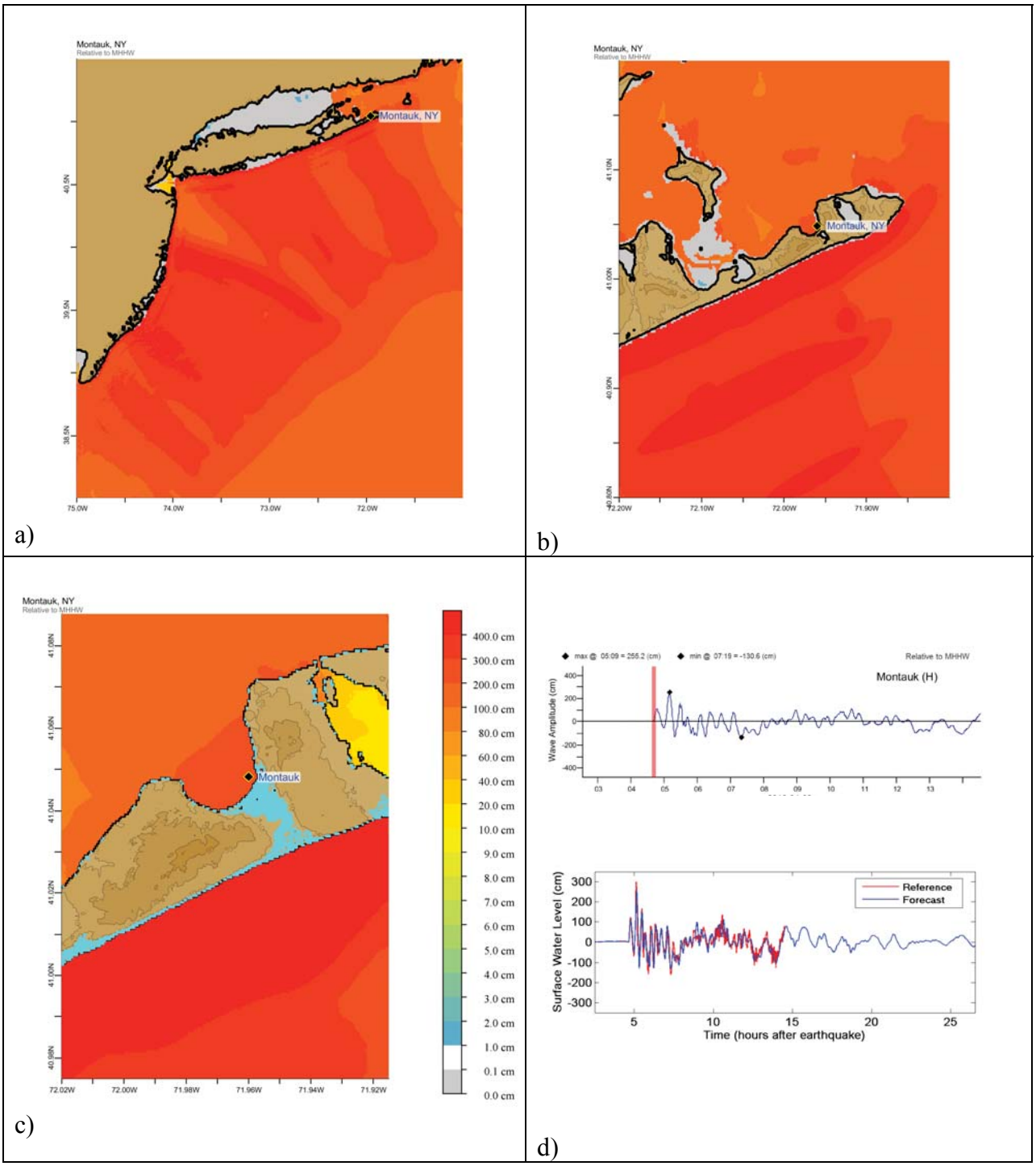

Figure C.2. Response of the Montauk forecast model to synthetic scenario ATSZ 48-57 (alpha=25). Maximum sea surface elevation for (a) A grid, b) B grid, c) C grid. Sea surface elevation time series at the C grid warning point (d). The lower time series plot is the result obtained during model development and is shown for comparison with test results.

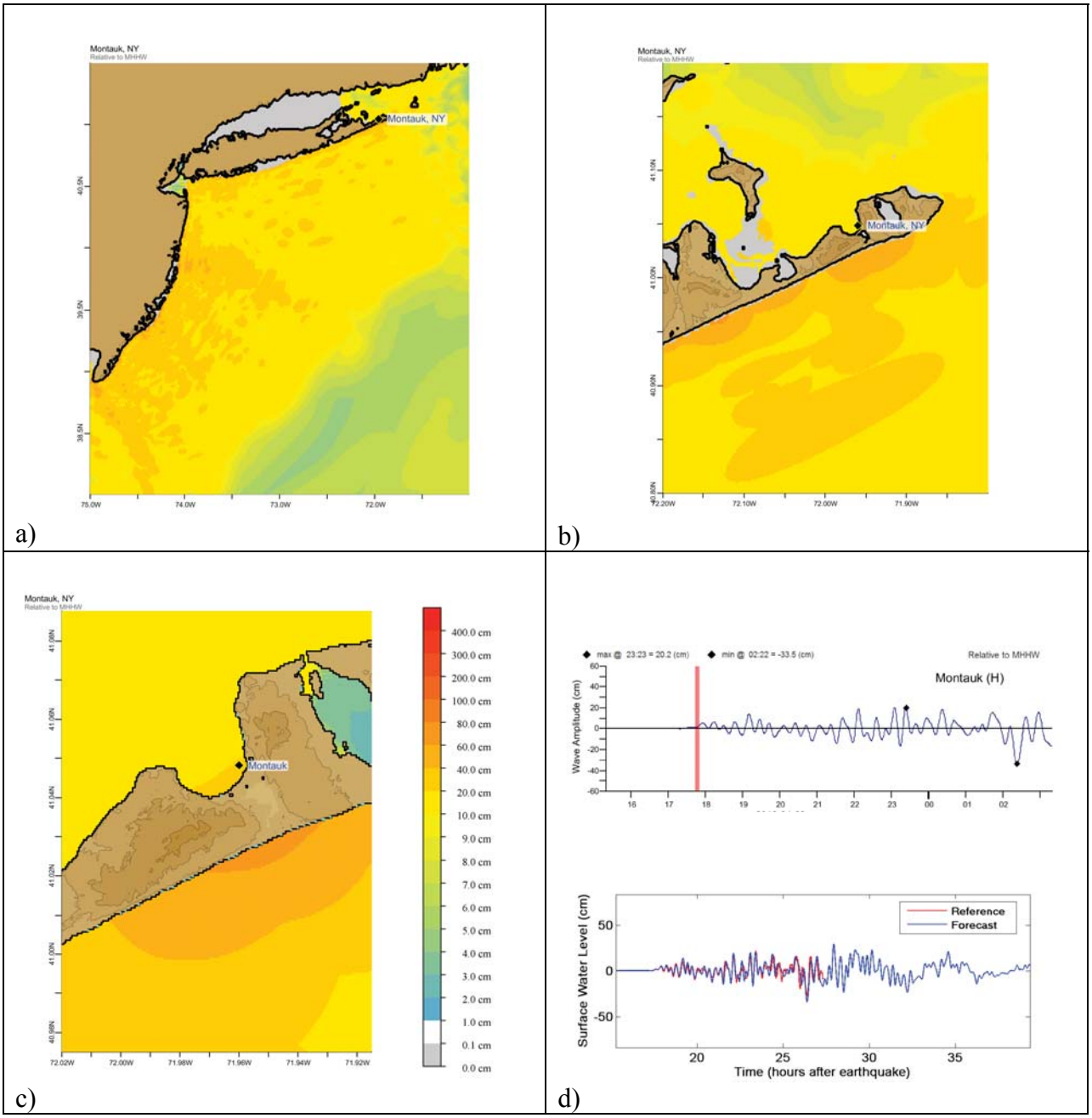

Figure C.3. Response of the Montauk forecast model to synthetic scenario SSSZ 1-10 (alpha=25). Maximum sea surface elevation for (a) A grid, b) B grid, c) C grid. Sea surface elevation time series at the C grid warning point (d)

Table C.1. Table of maximum and minimum amplitudes (cm) at the Montauk, New York, warning point for synthetic and historical events tested using SIFT 3.2 and obtained during development.

Scenario Name	Source Zone	Tsunami Source	α [m]	SIFT Max (cm)	Development Max (cm)	SIFT Min (cm)	Development Min (cm)
Mega-tsunami Scenarios							
ATSZ 38-47	Atlantic	A38-A47, B38-B47	25	53.4	53.44	-63.7	-63.55
ATSZ 48-57	Atlantic	A48-A57, B48-B57	25	255.2	255.24	-130.6	-130.60
SSSZ 1-10	South Sandwich	A1-A10, B1-B10	25	20.2[1]	29.49[1]	-33.5	-33.51

[1] The SIFT max is based on a 10-hr simulation while the development max is based on a 24-hr simulation. The higher value of development max is attributed to the arrival of later waves (beyond 10 hours).